

1 Serotonergic Psychedelics LSD & Psilocybin Increase the  
2 Fractal Dimension of Cortical Brain Activity in Spatial and  
3 Temporal Domains

4 TF Varley<sup>1,2,5\*</sup>, R Carhart-Harris<sup>3</sup>, Leor Roseman<sup>3,4</sup>, David K Menon<sup>1</sup>, EA Stamatakis<sup>1,2</sup>

5 January 16, 2019

6 <sup>1</sup> Division of Anaesthesia, School of Clinical Medicine, University of Cambridge, UK

7 <sup>2</sup> Department of Clinical Neurosciences, School of Clinical Medicine, University of Cambridge,  
8 UK

9 <sup>3</sup> Centre for Neuropsychopharmacology, Department of Medicine, Imperial College London, Lon-  
10 don, UK

11 <sup>4</sup> Computational, Cognitive and Clinical Neuroscience Laboratory, Department of Medicine,  
12 Imperial College London, London, UK

13 <sup>5</sup> Department of Psychological & Brain Sciences, Indiana University, Bloomington, IN, USA

14 \* Corresponding author E-mail: tvarley@iu.edu

15

## Abstract

16

17

18

19

20

21

22

23

24

25

26

27

28

29

30

31

32

33

34

35

36

37

Psychedelic drugs, such as psilocybin and LSD, represent unique tools for researchers investigating the neural origins of consciousness. Currently, the most compelling theories of how psychedelics exert their effects is by increasing the complexity of brain activity and moving the system towards a critical point between order and disorder, creating more dynamic and complex patterns of neural activity. While the concept of criticality is of central importance to this theory, few of the published studies on psychedelics investigate it directly, testing instead related measures such as algorithmic complexity or Shannon entropy. We propose using the fractal dimension of functional activity in the brain as a measure of complexity since findings from physics suggest that as a system organizes towards criticality, it tends to take on a fractal structure. We tested two different measures of fractal dimension, one spatial and one temporal, using fMRI data from volunteers under the influence of both LSD and psilocybin. The first was the fractal dimension of cortical functional connectivity networks and the second was the fractal dimension of BOLD time-series. We were able to show that both psychedelic drugs significantly increased the fractal dimension of functional connectivity networks, and that LSD significantly increased the fractal dimension of BOLD signals, with psilocybin showing a non-significant trend in the same direction. With both LSD and psilocybin, we were able to localize changes in the fractal dimension of BOLD signals to brain areas assigned to the dorsal-attentional network. These results show that psychedelic drugs increase the fractal character of activity in the brain and we see this as an indicator that the changes in consciousness triggered by psychedelics are associated with evolution towards a critical zone.

**Keywords:** Complexity, Consciousness, Criticality, Entropy, fMRI, Fractal, LSD, Networks, Psilocybin, Psychedelic

## 38 **Author Summary**

39 The unique state of consciousness produced by psychedelic drugs like LSD and psilocybin (the  
40 active component in magic mushrooms) are potentially useful tools for discovering how specific  
41 changes in the brain are related to differences in perception and thought patterns. Past research  
42 into the neuroscience of psychedelics has led to the proposal of a general theory of brain function and  
43 consciousness: the Entropic Brain Hypothesis proposes that consciousness emerges when the brain is  
44 sitting near a critical tipping point between order and chaos and that the mind-expanding elements  
45 of the psychedelic experience are caused by the brain moving closer to that critical transition point.  
46 Physicists have discovered that near this critical point, many different kinds of systems, from magnets  
47 to ecosystems, take on a distinct, fractal structure. Here, we used two measures of fractal-quality  
48 of brain activity, as seen in fMRI, to test whether the activity of the brain on psychedelics is more  
49 fractal than normal. We found evidence that this is the case and interpret that as supporting the  
50 theory that, psychedelic drugs are move the brain towards a more critical state.

## 51 1 Introduction

52 Since the turn of the century, there has been a renewal of interest in the science of serotonergic  
53 psychedelic drugs (LSD, psilocybin, mescaline, etc.), both in terms of possible medical applications  
54 of these drugs [1, 2], and what they might tell us about the relationship between activity in the  
55 brain and the phenomenological perception of consciousness [3, 4]. For those interested in the  
56 relationship between activity in the brain and consciousness, psychedelic drugs are particularly  
57 useful, as volunteers under the influence of a psychedelic are still able to report the nature of their  
58 experience and recall it even after returning to normal consciousness. This contrasts favourably  
59 with the other class of drugs commonly used to explore consciousness: anaesthetics, which by the  
60 very nature of their effects, make it difficult to gather first-person experiential data from a volunteer  
61 [5]. The subjective experience of the psychedelic state is associated with radical alterations to  
62 both internal and external senses, including visual distortions, vivid, complex closed-eye imagery,  
63 alterations to the sense of self, emotional extremes of euphoria and anxiety, and in extreme cases,  
64 psychosis-like effects [6]. The psychedelic experience can also have profound personal, and even  
65 spiritual or religious character [7, 8], which has made them central to the religious practices of many  
66 cultures around the world [9]. In this way, the study of the psychedelic state can inform not just  
67 the question of why consciousness emerges, but also the origins of some of the most quintessentially  
68 human psychological experiences.

69 Neuroimaging studies using fMRI and MEG have suggested that the experiential qualities of  
70 the psychedelic state can be explained, in part, by the effects these drugs have on the entropy of  
71 brain activity: a theory known as the Entropic Brain Hypothesis (EBH) [10, 4]. The EBH posits  
72 that during normal waking consciousness, activity in the brain is near, but slightly below, a critical  
73 zone between order and disorder, and that under the influence of psychedelic drugs the entropy  
74 of brain activity increases, bringing the system closer to the zone of criticality. In this context,  
75 'criticality' can be thought of as similar to a phase-transition between two qualitatively different  
76 states: the sub-critical state, which is comparatively inflexible, highly ordered and displays low  
77 entropy, while the super-critical state may be highly entropic, flexible, and disorganized (this recalls a  
78 canonical model of critical processes, the Ising Model, where the critical temperature divides distinct

79 phases, one where the magnetic spins are all aligned, and another where the spins are distributed  
80 chaotically, for review see [11]). The EBH is related to a larger theory of consciousness, known  
81 as Integrated Information Theory (IIT), which posits that consciousness is an emergent property  
82 of the integration of information in the brain [12, 13, 14] and that this mathematical formalism is  
83 categorically isomorphic to consciousness itself [15].

84 While it is currently impossible to directly measure the entropy of all of the activity in the whole  
85 of the brain, or the amount of information integration, there is much interest in using mathematical  
86 analysis of neuroimaging data to estimate the complexity of activity in the brain and relate that  
87 to consciousness. Studies with psilocybin have found that the patterns of functional connectivity  
88 in the brain undergo dramatic reorganization, characterized primarily by the rapid emergence and  
89 dissolution of unstable communities of interacting brain regions that do not occur in normal waking  
90 consciousness [16]. Similarly, under psilocybin, the repertoire of possible states functional connec-  
91 tivity networks can occupy is increased, which is interpreted as an increase in the entropy of the  
92 entire system [17]. Work on other psychedelics with pharmacology related to psilocybin has found  
93 similar results: under the influence of Ayahuasca, a psychedelic brew indigenous to the Amazon, the  
94 Shannon entropy of the degree distribution of functional connectivity networks is increased relative  
95 to normal consciousness [18] (encouragingly, the opposite effect has been shown under the conditions  
96 of sedation with propofol [19]). Analysis of MEG data from volunteers under the influence of lysergic  
97 acid diethylamide (LSD) has been shown an increase in the Lempel-Ziv complexity of the signals,  
98 which is thought to reflect increased complexity of activity in the brain [20]. LSD has also been  
99 recently shown to alter the connectome harmonics of brain networks, in a manner that suggests an  
100 increase in the complexity of network harmonics describing brain activity [21]. For a comprehensive  
101 review of the current state of psychedelic research into the EBH see *The Entropic Brain - Revisited*  
102 [4].

103 While a core element of the EBH is the theory that the psychedelic experience moves the brain  
104 closer to the zone of criticality, many of the measures that have been tested so far do not address  
105 the phenomena of criticality directly. These measures usually test where the brain falls on a unidi-  
106 mensional axis of order vs. randomness. Lempel-Ziv complexity [20], nodal entropy [18, 19] and the  
107 entropy of possible states [17], all describe a movement towards increased randomness and disorder,

108 which is consistent with the entropic predictions of the EBH, but not necessarily informative about  
109 the relative proximity to the zone of criticality. In these analyses, a completely random system  
110 would score maximally high on complexity (for instance a completely random time-series would  
111 have a normalized Lempel-Ziv score of unity, which is the upper bound of the measure) however it  
112 is nearly impossible to imagine how a living brain could output totally random data, and such a  
113 brain would most likely not be conscious. While these analyses are interesting and have clearly been  
114 fruitful, they paint a limited picture of the brain as a complex system, and don't directly test the  
115 central thesis of the EBH. To date, the only study that has directly addressed the criticality aspect  
116 of the EBH is the study of LSD and connectome harmonics [21], although other studies have found  
117 evidence of scale-free, power-law behaviour generally thought to be indicative of critical phenomena  
118 [22]. To address the relative lack of studies testing criticality directly, in this paper, we propose the  
119 fractal dimension of brain activity as a novel measure of complexity that provides insights into the  
120 criticality of the psychedelic state, as well as providing a measure of 'complexity' that is related to,  
121 but distinct from, the entropic measures described above.

122 Fractals are ubiquitous in nature and dramatic visualizations of colourful constructs like the  
123 Mandelbrot set have even permeated popular culture [23]. Psychedelic culture in particular shows  
124 a strong affinity for fractal patterns, as much of the imagery experienced under the influence of  
125 psychedelics is described as fractal in character. Fractals are defined by the property of having a  
126 non-integer dimension, which can be naively thought of as how 'rough' or 'complex' the shape in  
127 question is, or slightly more formally, the extent to which it maintains symmetry across different  
128 scales [24]. This is commonly known as 'self-similarity,' and can be intuitively understood as the  
129 invariance of appearance across scales: for example, the pattern of small creeks flowing together can  
130 resemble the pattern of large rivers carrying orders of magnitude more water [25]. In systems that  
131 display self-organizing criticality, as the system naturally evolves towards a critical point, its spatial  
132 structure will tend to take on increasingly fractal character that can be described in terms of fractal  
133 dimension [26, 27, 28], and in systems which can be 'tuned' to a critical state (such as the Ising model,  
134 which has been explored as a model of critical brain activity [29, 30, 31]), fractal structures emerge  
135 near the critical point [32]. If, under the influence of a psychedelic, the brain is moving closer towards  
136 a state of criticality, as the EBH posits, then we might expect any fractal character in brain activity

137 to become more pronounced. There is some evidence of a symmetrical effect when consciousness is  
138 lost: in states of sleep and drug-induced anaesthesia, the fractal dimension of brain activity drops  
139 significantly, with the exception of REM sleep, during which the fractal dimension rises again [33, 34].  
140 As REM sleep is the state of sleep when the greatest quantity of phenomenological experience takes  
141 place (in the form of dreams), this suggests that the fractal dimension of brain activity is related  
142 to the 'quantity' of experiential consciousness available to an individual. Similarly, in rats, during  
143 ketamine-induced anaesthesia the fractal dimension of brain activity is significantly higher in key-  
144 brain regions associated with consciousness when compared with anaesthesia induced by other drugs  
145 [35], and as ketamine is known to induce vivid, dream-like states of consciousness at high doses [36],  
146 which comports with the REM sleep finding.

147 There has been considerable interest in applying techniques of fractal analysis to questions in  
148 neuroscience and considerable evidence has mounted that both the physical structure of the brain  
149 itself, and the patterns of activity measured by neuroimaging paradigms display pronounced fractal  
150 character [37, 38]. Changes to the fractal dimension of brain structures are associated with changes  
151 in cognition and clinically significant diagnosis, such as schizophrenia and obsessive-compulsive dis-  
152 order [39], intelligence [40], Alzheimer's disease [41], and ageing [42]. There is some preliminary  
153 evidence that cortical functional connectivity networks display fractal character, both during rest  
154 and tasks [43] and that this fractal character plays an important role in regulating how information  
155 is propagated through the brain [44].

156 While fractal dimension is usually thought to encode complexity in terms of self-similarity rather  
157 than entropy directly, there is a connection between the two values: fractal dimension is related  
158 to Renyi entropy, which is itself a generalization of the classical measure of Shannon entropy [45].  
159 Computational models have shown that as the fractal dimension of a shape rises, so does the associ-  
160 ated Renyi entropy [46]. Another measure, the information dimension, relates the fractal dimension  
161 to the information content of a fractal at different scales [47, 48]. Based on these findings, and the  
162 results reported by Bak et al., (1987), we propose that the fractal dimension is a natural metric by  
163 which to test the EBH, for several reasons. First, unlike other metrics of entropy, fractals are inti-  
164 mately related to the phenomena of criticality, which is predicted to be significant for consciousness,  
165 and the fractal dimension encodes information relevant to a system's evolution towards criticality.

166 Second, in this context, they are a novel method of describing the behaviour of the brain as a com-  
167 plex system and so give information beyond the axis of order versus randomness. Finally, despite  
168 the differences between the measure of fractal dimension and classical entropy, the two are related  
169 in some fundamental ways. The fractal dimension sits at a sweet spot of not being so radical that  
170 it cannot be related to previous results, while still being novel enough to open the door to new and  
171 informative avenues of study.

172 To test the relationship between the fractal dimension of activity of brain and consciousness,  
173 we used fMRI data from subjects under the influence of either LSD or psilocybin, provided by the  
174 Psychedelic Research Group at Imperial College London. From this data, we created 1000-node  
175 functional connectivity networks and performed a network-specific variation of the box-counting  
176 algorithm [49] to extract the fractal dimension. We also used a second measure, the Higuchi fractal  
177 dimension [50], to test the temporal fractal dimension of BOLD time-series. These two measures  
178 capture two axes on which the complexity of brain activity might be measured: spacial (network  
179 fractal dimension) and temporal (Higuchi fractal dimension). If the psychedelic state is associated  
180 with a movement towards a critical zone associated with increased fractal character, we would  
181 expect to see this when examined on multiple measures, and so these two measures serve as internal  
182 validation for each-other. While the network fractal dimension is not spacial in the way, for example,  
183 a 2-dimensional box-counting analysis of activity at the cortical surface would be, it does return  
184 insight into how information processing may be distributed across multiple, spatially distinct brain  
185 regions.

## 186 **2 Materials & Methods**

### 187 **2.1 Ethics Statement**

188 The data analyzed here have been reported in previous studies [59, 58]. Both studies described herein  
189 were approved by a UK National Health Service research ethics committee, and the researchers  
190 complied with all relevant regulations and ethical guidelines, including data privacy and participant  
191 informed consent.



## 192 2.2 Calculating Network Fractal Dimension

193 When calculating the fractal dimension of a naturally occurring system, researchers commonly use a  
194 box-counting algorithm, which is an accessible and computationally tractable method that captures  
195 the distribution of elements across multiple scales [24]. Intuitively, the box-counting dimension  
196 defines the relationship between a measured quality of a shape in space, and the metric used to  
197 measure it. The canonical example is the question of how long the coastline of Britain is [51].  
198 If one wishes to measure the length of Britain's coast, they could estimate it by calculating the  
199 number of square boxes  $N_B(l_B)$ , of a given width  $l_B$ , that are necessary to tile the entire coastline.  
200 For very large values of  $l_B$ ,  $N_B(l_B)$  will be small, while as the value of  $l_B$  decreases,  $N_B(l_B)$  will  
201 asymptotically approach some value. If the shape being tiled is a fractal, then:

$$N_B(l_B) \propto l_B^{-d_B} \quad (1)$$

202 Where  $d_B$  is the box-counting dimension. Algebraic manipulation shows that  $d_B$  can be extracted  
203 by linear regression in log-log space as:

$$\lim_{l_B \rightarrow 1} \frac{\ln(N_B(l_B))}{\ln(l_B)} \propto -d_B \quad (2)$$

204 A similar logic is used when calculating the box-counting dimension of a graph. For a graph  
205  $G = (V, E)$ , a box with diameter  $l_B$  defines a set of nodes  $B \subset V$  where for every pair of nodes  
206  $v_i$  and  $v_j$  the distance between them  $l_{ij} < l_B$ . Here, the distance between two nodes  $v_i, v_j$  is the  
207 graph geodesic between the vertices: the number of edges in the shortest path between them. To  
208 quantify the fractal dimension of the functional connectivity networks, a box counting method, the  
209 Compact Box Burning algorithm (CBB) [49], was used to find  $N_B(l_B)$  for a range of integer  $l_B$   
210 values 1..10. If  $G$  has fractal character, a plot of  $\ln(N_B(l_B))$  vs.  $\ln(l_B)$  should be roughly linear,  
211 with a slope of  $-d_B$ . Unfortunately, because of the logarithmic relationship between box-size and  
212 fractal dimension, exponentially higher resolutions are required to achieve modest increases in the  
213 accuracy of the measured fractal dimension. Computational explorations, where a box-counting  
214 method is used to approximate a fractal dimension that has already been solved analytically, show  
215 that the box-counting dimension converges to the true dimension with excruciating slowness [52],

216 necessitating the highest-resolution parcellation that is computationally tractable.

217 It should be noted that there has been much discussion surrounding the appropriateness of this  
218 method for describing the presence (or absence) of power-laws in empirical data [53]. We chose the  
219 above-described method for a few reasons: the first was to remain as consistent as possible with the  
220 method used in previous analysis of the fractal dimension of human FC networks [44, 43], the second  
221 was because of the tractability of the analysis, and finally, the relatively small size of the network  
222 forced a limited range of box sizes  $l_B$  (approximately a single order of magnitude), which precluded  
223 the use of larger, more data-driven analyses. We stress that, given the ongoing discussion around  
224 the optimal way to find power-law relationships, the results reported here should not be interpreted  
225 as an unambiguous claim of incontrovertible proof that such a power-law relationship holds here -  
226 rather a preliminary result to establish the possibility that fractal topologies and brain dynamics  
227 may be related to the maintenance of consciousness.

228 The implementation of the CBB was provided as open-source code by the Mackse lab, and can  
229 be found at: <http://www-levich.engr.cuny.cuny.edu/webpage/hmakse/software-and-data/>

### 230 **2.3 Calculating BOLD Time-Series Fractal Dimension**

231 To calculate the temporal fractal dimension, we used the Higuchi method for calculating the self-  
232 similarity of a one-dimensional time-series, an algorithm widely used in EEG and MEG analysis [54].  
233 The original method is recorded in detail in the original paper [50], but will be briefly described  
234 here. The algorithm takes in a time-series  $X(t)$  with  $N$  individual samples, defined as:

$$X(t) = x_1, x_2, x_3, \dots, x_N \quad (3)$$

235 In this case, every  $X(t)$  corresponds to one Hilbert-transformed BOLD time-series  $H(t)$  extracted  
236 from our functional brain scans (details below). Hilbert-transforming was chosen to be consistent  
237 with previously-reported studies of time-series complexity and consciousness [55, 56, 20]. From each  
238 time-series  $X(t)$ , we create a new time-series  $X(t)_k^m$ , defined as follows:

$$X(t)_k^m = x_m, x_{m+k}, x_{m+2k}, \dots, x_{m+\lfloor \frac{N-m}{k} \rfloor k} \quad (4)$$

239 where  $m = 1, 2, \dots, k$ .

240 For each time-series  $X(t)_k^m$  in  $k_1, k_2, \dots, k_{max}$ , the length of that series,  $L_m(k)$ , is given by:

$$L_m(k) = \frac{(\sum_{i=1}^{\lfloor \frac{N-m}{k} \rfloor} |x_{im+k} - x_{(i-1)k}|) \frac{N-1}{\lfloor \frac{N-m}{k} \rfloor k}}{k} \quad (5)$$

241 We then define the average length of the series  $\langle L(k) \rangle$ , on the interval  $[k, L_m(k)]$  as:

$$\langle L(k) \rangle = \sum_{m=1}^k \frac{L_i(k)}{k} \quad (6)$$

242 If our initial time-series  $X(t)$  has fractal character, then  $\langle L(k) \rangle \propto k^{-D}$ . As with the procedure for  
243 calculating the network fractal dimension, the algorithm iterates through values of  $k$  from  $1 \dots k_{max}$   
244 and calculates  $\ln(\langle L(k) \rangle)$  vs.  $\ln(k^{-1})$ , extracting  $D$  by linear regression. The various values of  $k$   
245 can be thought of as analogous to the various values of  $l_B$  used to calculate the network fractal  
246 dimension. The Higuchi algorithm requires a pre-defined  $k_{max}$  value as an input, along with the  
247 target time-series. This value is usually determined by sampling the results returned by different  
248 values of  $k_{max}$  and selecting a value based on the range of  $k_{max}$  where the fractal dimension is stable.  
249 For the psilocybin and LSD datasets, we sampled over a range of powers of two ( $2, \dots, 128$ ). Due to  
250 the comparably small size of BOLD time-series (100 entries for the psilocybin dataset and 434 entries  
251 for the LSD dataset), the range of  $k_{max}$  values that our algorithm could process without returning  
252 an error was limited. We ultimately decided on  $k_{max} = 64$  for the LSD dataset and  $k_{max} = 32$  for  
253 the psilocybin dataset.

254 The implementation we used was from the PyEEG toolbox [57], downloaded from the Anaconda  
255 repository.

## 256 2.4 Data Acquisition & Preprocessing

257 Both the LSD data and the psilocybin data were provided by the Psychedelic Research Group at  
258 Imperial College London, having already been preprocessed according to their specifications.

#### 259 **2.4.1 LSD Data**

260 The data acquisition protocols and preprocessing pipelines were described in detail in a previous  
261 paper [58], so we will describe them in brief here. 20 healthy volunteers underwent two scans, 14 days  
262 apart. On one day they were given a placebo (10-mL saline) and on the other they were given an  
263 active dose of LSD (75  $\mu$ g of LSD in 10-mL saline). BOLD scanning consisted of three seven minute  
264 eyes closed resting state scans. The first and third scans were eyes-closed, resting state without any  
265 in-ear auditory stimulation (music), and these were what were used in this report.

266 Anatomical imaging was performed on a 3T GE HDx system. These were 3D fast spoiled gradient  
267 echo scans in an axial orientation, with field of view =  $256 \times 256 \times 192$  and matrix =  $256 \times 256 \times 129$   
268 to yield 1mm isotropic voxel resolution. TR/TE = 7.9/3.0ms; inversion time = 450ms; flip angle  
269 =  $20^\circ$  BOLD-weighted fMRI data were acquired using a gradient echo planer imaging sequence,  
270 TR/TE = 2000/35ms, FoV = 220mm,  $64 \times 64$  acquisition matrix, parallel acceleration factor = 2,  
271  $90^\circ$  flip angle. Thirty five oblique axial slices were acquired in an interleaved fashion, each 3.4mm  
272 thick with zero slice gap (3.4mm isotropic voxels). The precise length of each of the two BOLD  
273 scans was 7:20 minutes. One subject aborted the experiment due to anxiety and four others were  
274 excluded for excessive motion (measured in terms of frame-wise displacement).

275 The following pre-processing stages were performed: removal of the first three volumes, de-  
276 spiking (3dDespike, AFNI), slice time correction (3dTshift, AFNI), motion correction (3dvolreg,  
277 AFNI) by registering each volume to the volume most similar to all others, brain extraction (BET,  
278 FSL); 6) rigid body registration to anatomical scans, non-linear registration to 2mm MNI brain  
279 (Symmetric Normalization (SyN), ANTS), scrubbing (FD = 0.4), spatial smoothing (FWHM) of  
280 6mm, band-pass filtering between [0.01 to 0.08] Hz, linear and quadratic de-trending (3dDetrend,  
281 AFNI), regressing out 9 nuisance regressors (all regressors were bandpass-filtered using the same  
282 range described above).

#### 283 **2.4.2 Psilocybin Data**

284 The data acquisition protocols and preprocessing pipelines were described in detail in a previous  
285 paper [59], so we will describe them in brief here. Fifteen healthy volunteers were scanned. Anatom-  
286 ical and task-free resting state scans (each lasting 18 minutes) were taken. Solutions were infused

287 manually over 60 s, beginning 6 min after the start of each functional scan. Subjects psilocybin  
288 (2 mg in 10-mL saline) in the active scan. In this study we used only the psilocybin-positive scan,  
289 comparing the pre-infusion condition to the post-infusion condition for control.

290 All imaging was performed on a 3T GE HDx system. For every functional scan, we obtained  
291 an initial 3D FSPGR scan in an axial orientation, with FoV =  $256 \times 256 \times 192$  and matrix =  
292  $256 \times 256 \times 192$  to yield 1-mm isotropic voxel resolution (TR/TE = 7.9/3.0 ms; inversion time = 450  
293 ms; flip angle =  $20^\circ$ ). BOLD-weighted fMRI data were acquired using a gradient-echo EPI sequence,  
294 TR/TE 3000/35 ms, field-of-view = 192 mm,  $64 \times 64$  acquisition matrix, parallel acceleration factor  
295 = 2,  $90^\circ$  flip angle. Fifty-three oblique-axial slices were acquired in an interleaved fashion, each 3  
296 mm thick with zero slice gap ( $3 \times 3 \times 3$ -mm voxels). A total of 240 volumes were acquired.

297 All data was preprocessed using the following pipeline: de-spiking, slice time correction, motion  
298 correction to best volume, brain extraction using the BET module in FSL, registration to anatomy  
299 (using FSL BBR), registration to 2mm MNI (ANTS), scrubbing (FD=0.4), smoothing with a 6mm  
300 kernel, bandpass filtering [0.01-0.08 Hz], linear and quadratic detrending, regression of 6 motion  
301 regressors and 3 nuisance regressors (all of the regressors were not smoothed and were bandpassed  
302 with the same filters). At the suggestion of the original research team that provided the data, six  
303 volunteers were excluded from the analysis for excessive motion.

## 304 **2.5 Formation of Functional Connectivity Networks**

305 BOLD time-series data were extracted from each brain in CONN (CONN is a collection of SPM/MATLAB  
306 scripts with a GUI designed for easy manipulation of fMRI, MEG, and EEG data. It is available at  
307 <http://www.nitrc.org/projects/conn>) [60] and the cerebral cortex was segmented into 1000 distinct  
308 ROIs, using the "Schaefer Local/Global 1000 Parcellation" [61] ([https://github.com/ThomasYeoLab/CBIG/blob/master](https://github.com/ThomasYeoLab/CBIG/blob/master/Schaefer2018_LocalGlobal/Parcellations/MNI/Schaefer2018_1000Parcels_7Networks_order_FSLMNI152_1mm.nii.gz)  
309 [/Schaefer2018\\_LocalGlobal/Parcellations/MNI/Schaefer2018\\_1000Parcels\\_7Networks\\_order\\_FSLMNI152\\_1mm.nii.gz](https://github.com/ThomasYeoLab/CBIG/blob/master/Schaefer2018_LocalGlobal/Parcellations/MNI/Schaefer2018_1000Parcels_7Networks_order_FSLMNI152_1mm.nii.gz))  
310 Due to the slow-convergence of Eq. 2, and the necessity of having a network with a wide enough  
311 diameter to accommodate a sufficiently wide range of box-sizes (if  $l_B$  is greater than or equal to the  
312 diameter of the network, then  $N(l_B)$  is trivially one), we attempted to strike an optimal balance  
313 between network resolution and computational tractability.

314 Every time-series  $F(t)$  was first transformed by taking the norm of the Hilbert transform of each

315 time-series, to ensure an analytic signal and keep the signals consistent with the Higuchi fractal  
316 dimension analysis.

$$H(t) = |\text{Hilbert}(F(t))| \quad (7)$$

317 Pearson Correlation was chosen largely due to it's wide use in the field and ease of interpretation.  
318 While more exotic, nonlinear similarity functions exist (normalized mutual information, information-  
319 based similarity, etc), for a prospective study of this sort, use of a well-characterized, linear function  
320 was appropriate, although future studies might explore the effect of different functions on large  
321 network topology. The resulting time-series  $H(t)$  was then correlated against every other time-  
322 series, using the Pearson Correlation, forming a matrix  $M$  such that:

$$M_{ij} = \rho(H_i(t), H_j(t)) \quad (8)$$

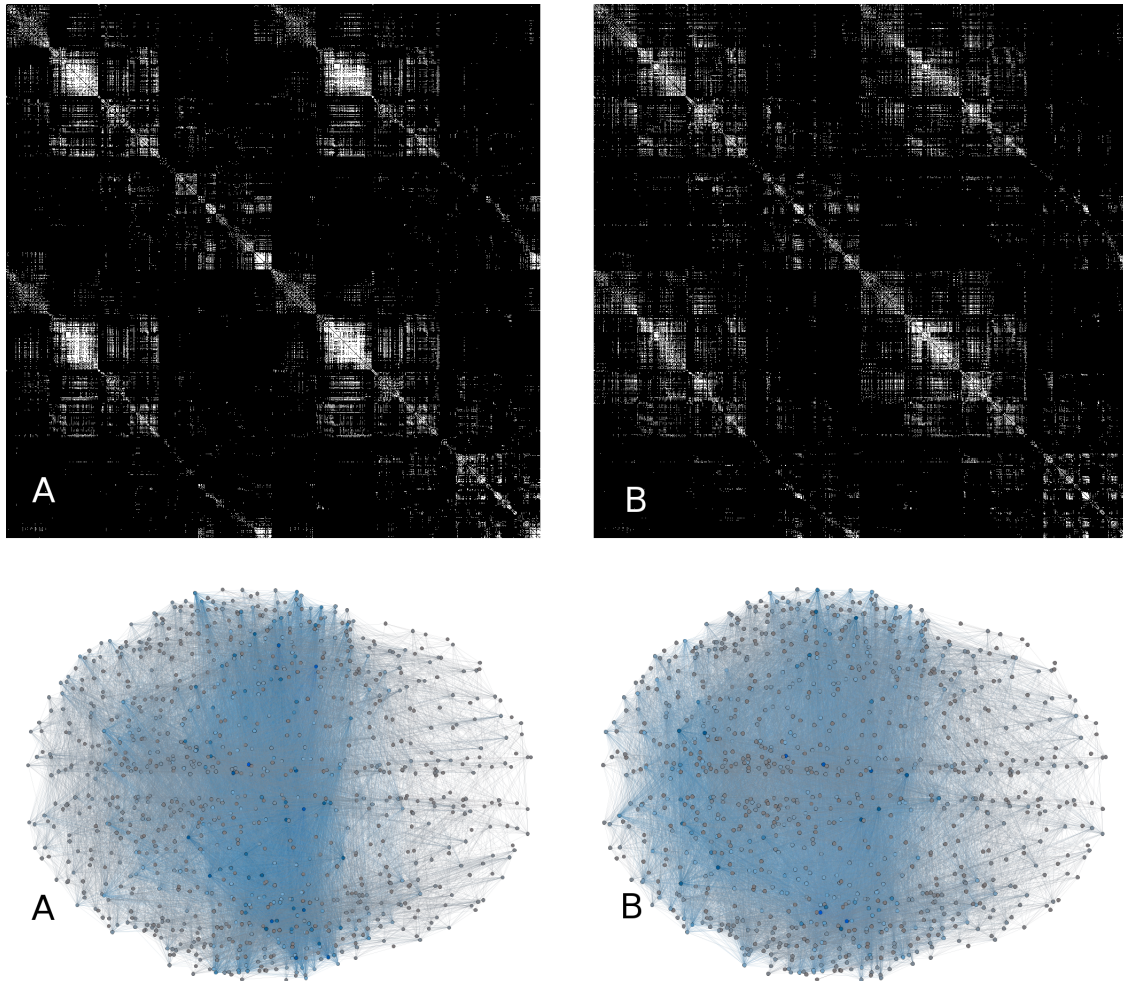
323 No significance testing was done (every  $\rho$  was included, regardless of whether it met some arbi-  
324 trary  $\alpha$  value or not), because significance filtering would result in an uneven distribution of edges  
325 and degrees between graphs that may have effected the analysis. Due to the high thresholding,  
326 the vast majority of weak, or potentially spurious connections were likely removed anyway. The  
327 correlation matrix has a series of ones that run down the diagonal, corresponding the correlation  
328 between each timeseries and itself which, if treated directly as a graph adjacency matrix, would  
329 produce a graph where each node had exactly one self-loop in addition to all it's other connections.  
330 To correct for this, the matrices were filtered to remove self-loops by turning the diagonal of ones  
331 to zeros, ensuring simple graphs:

$$M_{ij} = \begin{cases} 0, & \text{if } i = j \\ M_{ij}, & \text{otherwise} \end{cases} \quad (9)$$

332 Finally, the matrices were binarized with a 95% threshold, such that:

$$M_{ij} = \begin{cases} 1, & \text{if } M_{ij} \geq P_{95} \\ 0, & \text{otherwise} \end{cases} \quad (10)$$

333 The thresholding procedure was passed over all entries in the matrix, regardless of whether they  
334 were positive or negative, and any surviving edges became ones. The practical effect of such stringent  
335 thresholding is that only positive values survived, and including the negative values drove down the  
336 minimum edge weight that survived thresholding, resulting in a marginally less sparse network than  
337 what might have occurred if negative values had been thrown out prior to thresholding. While  
338 binarization does throw out information, the CBB algorithm that we used does not factor edge  
339 weight into whether two nodes constitute members of the same box. A 95% threshold was chosen  
340 based on the findings of Gallos et al., who showed that functional connectivity networks only display  
341 fractal character at high thresholds (see Introduction). All surviving values  $M_{ij} < 0 \mapsto 0$ . The results  
342 could then be treated as adjacency matrices defining functional connectivity graphs, where each row  
343  $M_i$  and column  $M_j$  corresponds to an ROI in the initial cortical parcellation, and the connectivity  
344 between all nodes is given by Eq. 3. To see samples of the binarized adjacency matrices, and the  
345 associated graphs see Figure 1.



**Whole-brain functional connectivity networks and matrices.**

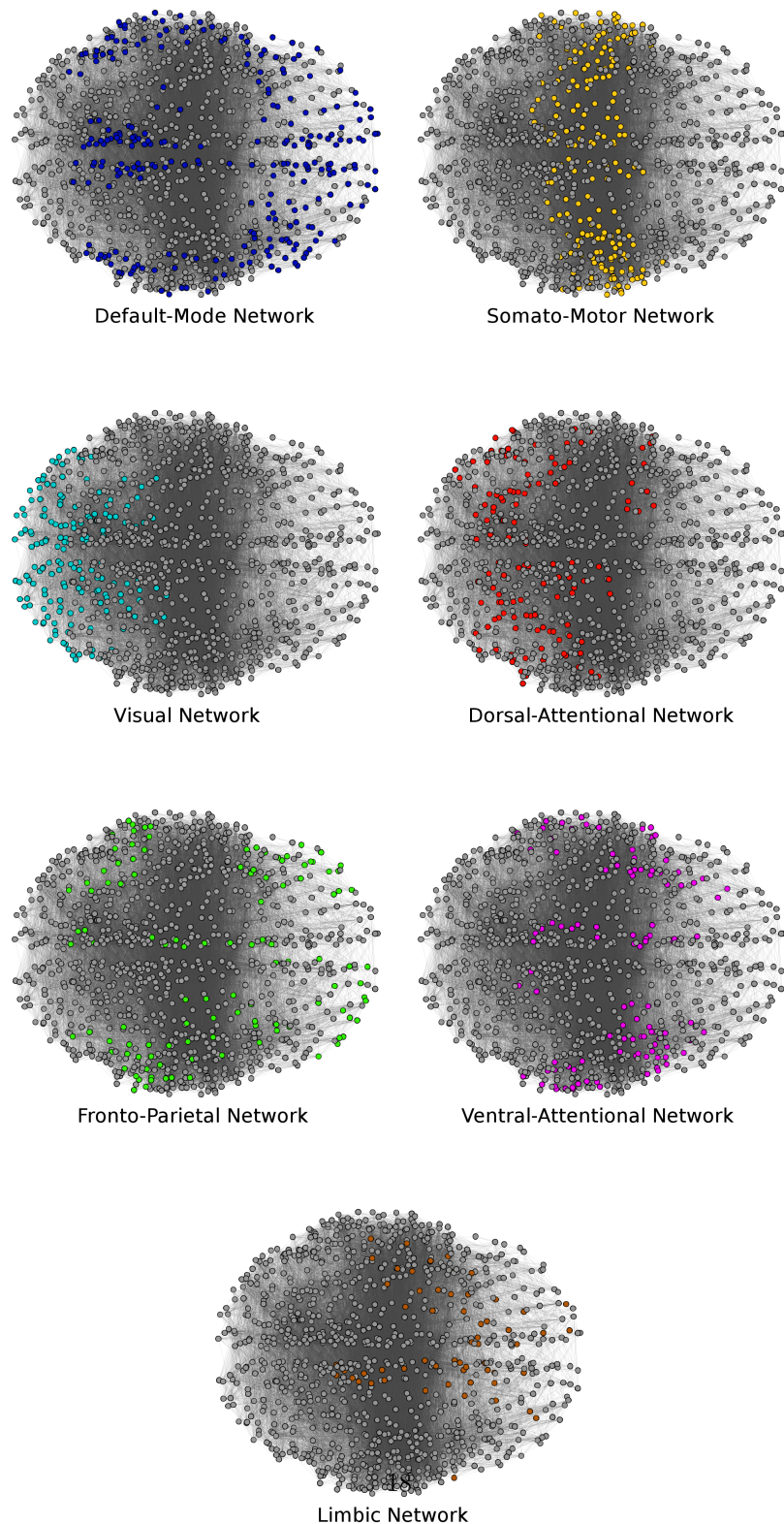
Figure 1: Two binarized, 1000-ROI adjacency matrices from a single subject, and their associated functional connectivity graphs ( $A \leftrightarrow A$ , etc). In the adjacency matrices, every pixel represents an edge between two nodes: if the pixel is white, the edge exists, if black, the edge does not exist. A is the functional connectivity matrix from the placebo condition, B is the matrix from the LSD condition. While the differences in fractal character are not intuitively obvious upon visual inspection, subtle differences in the distribution of connections can be seen.

When the corresponding networks are constructed, differences in gross-scale connectivity can be seen, although, as with the matrices, a change in fractal structure is not intuitively obvious. The networks are constructed using axial projections of the 3-dimensional atlas: each node is roughly at the centroid of it's associated ROI.



### 346 **2.5.1 Specific-Network Analysis**

347 To localize changes in the complexity of brain activity, individual ROIs were grouped into networks,  
348 using the mapping proposed by Yeo et al., [62]. We used the 1000 ROI parcellation with seven  
349 networks: default mode network, somato-motor network, visual network, dorsal-attentional network,  
350 ventral-attentional network, limbic network, and fronto-parietal control network. For visualization of  
351 the assignment of nodes to these networks see Figure 2. We then used the Higuchi fractal dimension  
352 method described above on each subset of regions to get a measure of the average time-series fractal  
353 dimension of each network.



### Assignment of nodes to canonical networks.

Figure 2: A visualization of how the 1000-node functional connectivity networks were parcellated into seven different brain regions, following the mapping described by Yeo et al., [62, 61]. The specific map file is available from GitHub at [https://github.com/ThomasYeoLab/CBIG/blob/master/stable\\_projects/brain\\_parcellation/Schaefer2018\\_LocalGlobal/Parcellations/MNI/Schaefer2018\\_1000Parcels\\_7Networks\\_order.txt](https://github.com/ThomasYeoLab/CBIG/blob/master/stable_projects/brain_parcellation/Schaefer2018_LocalGlobal/Parcellations/MNI/Schaefer2018_1000Parcels_7Networks_order.txt)

## 354 **2.5.2 Statistical Analysis**

355 All analysis was carried out using the Python 3.6 programming language in the Spyder IDE ([https://github.com/spyder-](https://github.com/spyder-ide/spyder)  
356 [ide/spyder](https://github.com/spyder-ide/spyder)), using the packages provided by the Anaconda distribution (<https://www.anaconda.com/download>).  
357 All packages were in the most up-to-date version, with the exception of NetworkX: due to compat-  
358 ibility issues with the CBB code, NetworkX v. 0.36 was used. Packages used include NumPy [63],  
359 SciPy [64], and NetworkX [65]. NetworkX was used for the implementation of the CBB algorithm,  
360 NumPy was used for manipulation of adjacency matrices and arrays, SciPy was used for statistical  
361 analysis, primarily using the SciPy.Stats module. Unless otherwise specified, all the significance tests  
362 are non-parametric: given the small sample sizes and heterogeneous populations, normal distribu-  
363 tions were not assumed. Wilcoxon Signed Rank test was used to compare drug conditions against  
364 their respective control conditions.

## 365 **3 Results**

### 366 **3.1 LSD & Psilocybin Network Fractal Dimension**

367 The Wilcoxon signed-rank test found significant differences, when corrected with the Benjamini-  
368 Hochberg procedure with an FDR of 5% [66], between LSD and placebo conditions ( $H(4)$ ,  $p$ -value  
369 = 0.001), and between the pre-infusion and post-infusion psilocybin conditions ( $H(6)$ ,  $p$ -value =  
370 0.05). The mean fractal dimensions for the LSD condition was  $3.37 \pm 0.15$ , and for the associated  
371 placebo condition it was  $2.939 \pm 0.29$ . For psilocybin the mean fractal dimension was  $3.52 \pm 0.049$ ,  
372 and for control it was  $3.277 \pm 0.372$ . For a plot of the relative fractal dimensions, see Figure 3. For  
373 a visualization for how the fractal dimension was calculated by linear regression for LSD see 4A and  
374 for Psilocybin, see Figure 4B.

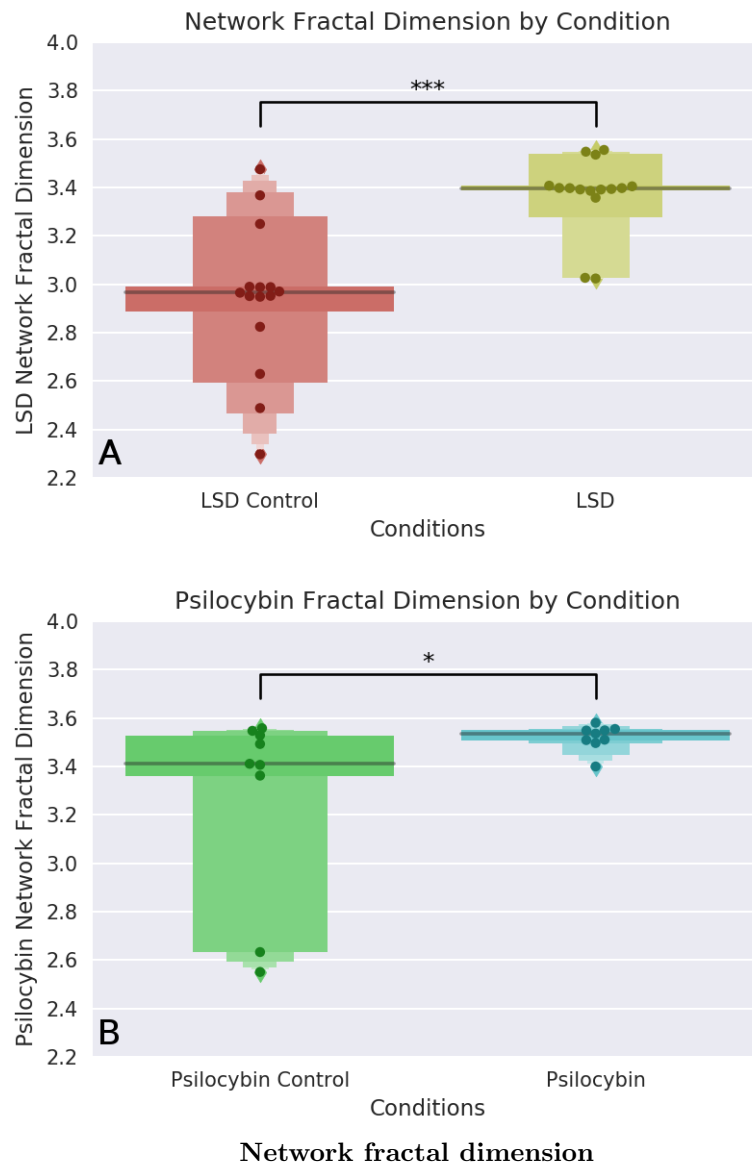
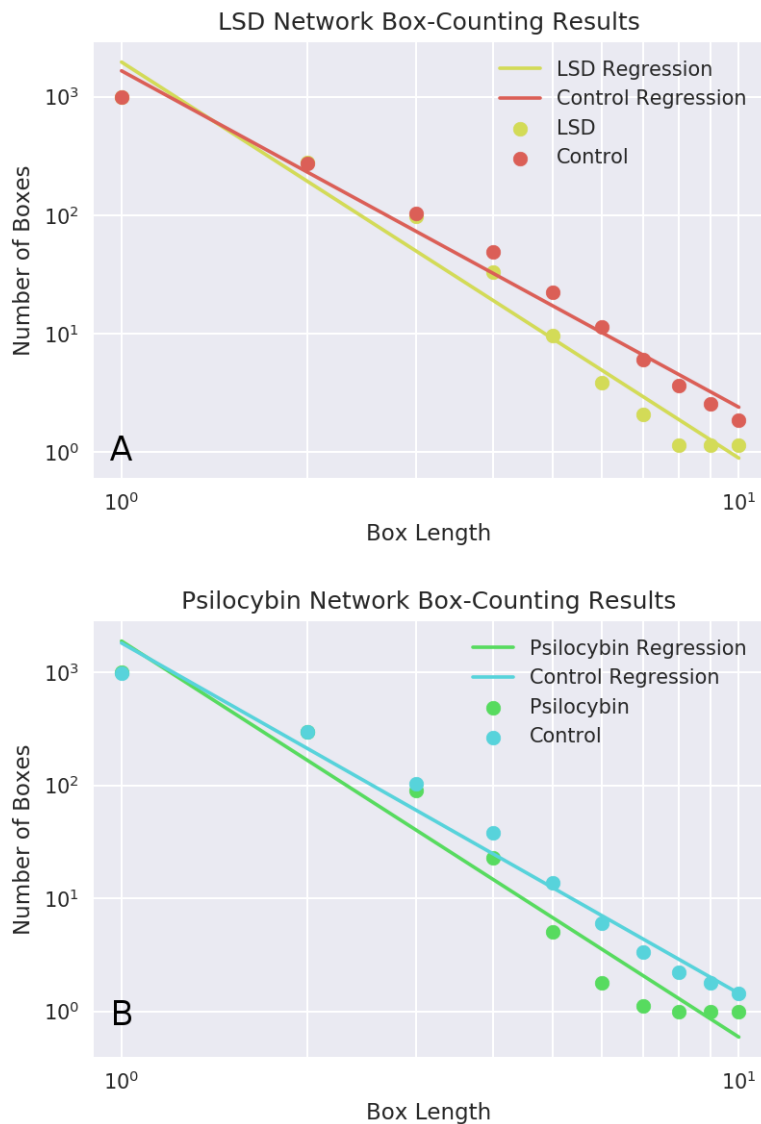


Figure 3: Letter-value plots of the network fractal dimensions for the two psychedelic drugs tested. Note that both psychedelic conditions show less variability compared to their respective controls.  
\*  $p \leq 0.05$ , \*\*  $p \leq 0.01$ , \*\*\*  $p \leq 0.001$



**Log-log regression of box length vs. number of boxes to tile the network.**

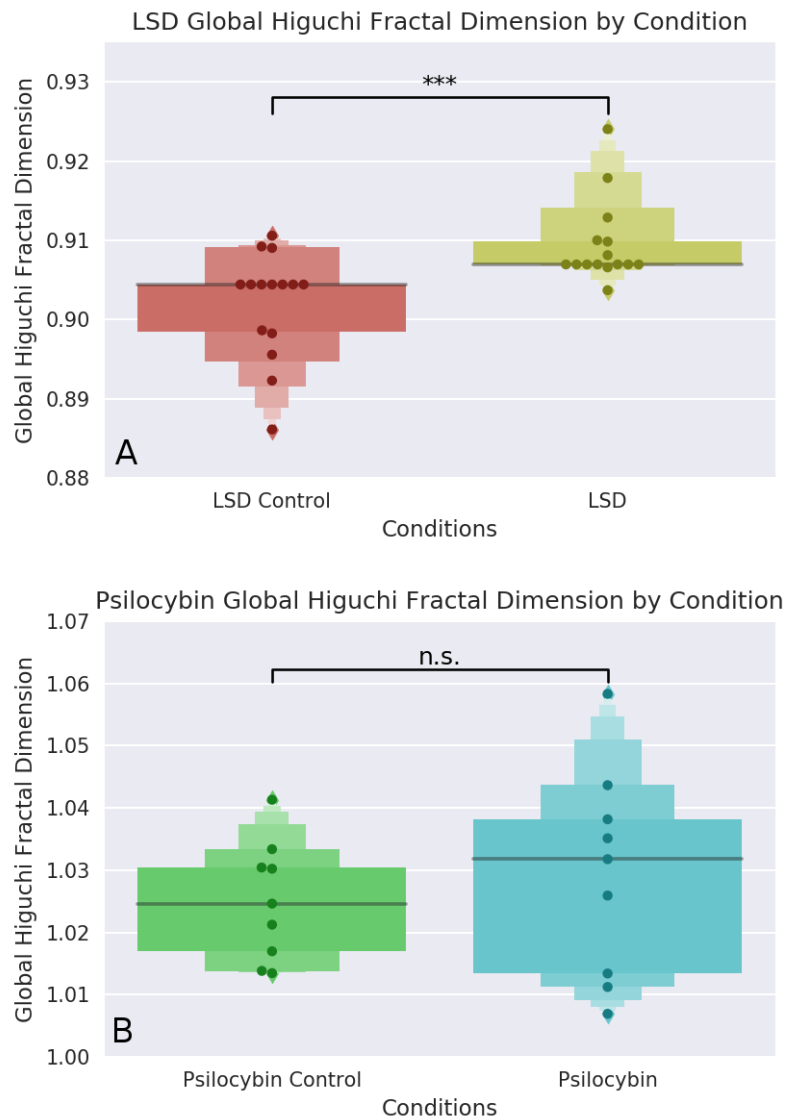
Figure 4: Here is the derivation of the fractal dimension for the LSD and psilocybin tests. For a range of integer-valued box-lengths ( $\{1,2,\dots,10\}$ ), the minimum number of boxes of that length necessary to tile a 1,000-ROI functional connectivity measure is calculated. If the log-transformed values display a linear relationship, that is evidence of a power-law distribution, and the slope characterizes the dimension of the network. Here, each point is the average number of boxes across all subjects ( $n=15$ ) in that condition, for each box length. A steeper slope corresponds to a higher fractal dimension, which is associated with a more complex system.

Note the log-log axes.

375 These results are consistent with the EBH, which posits that the properties of criticality will  
376 increase during psychedelic states [10]. These results are also consistent with the hypothesis that the  
377 changes in brain activity induced by LSD are very similar to the changes induced by psilocybin, which  
378 is unsurprising given their shared serotonergic pharmacology and the phenomenological similarities  
379 between the associated experiences. The difference in base-line fractal dimension [between LSD and  
380 psilocybin] is intriguing: we had expected it to be consistent across both datasets, as normal waking  
381 consciousness is presumably similar among volunteers in both datasets. We tentatively hypothesize  
382 that it may be a result of differences in data acquisition and processing specifications. It may  
383 be, however, that the base-line fractal dimension of BOLD signals is not as consistent between  
384 populations as we had assumed, and this may be an interesting future direction of exploration.

### 385 **3.2 LSD & Psilocybin BOLD Time-Series Fractal Dimension**

386 The Wilcoxon signed-rank test, when corrected with the Benjamini-Hochberg procedure with an  
387 FDR of 5%, found significant differences between the Higuchi fractal dimension of the LSD time-series  
388 and placebo time-series ( $H(3)$  p-value=0.001), but not between the pre-infusion and post-infusion  
389 psilocybin time-series. The mean network fractal dimension for the LSD-condition time-series was  
390  $0.91 \pm 0.005$  and for the placebo condition it was  $0.9 \pm 0.006$ . For the post-infusion psilocybin  
391 condition, the mean network fractal dimension of the BOLD time-series was  $1.03 \pm 0.015$ , while  
392 for the pre-infusion condition it was  $1.02 \pm 0.009$ . For visualization of the global Higuchi fractal  
393 dimension for the LSD versus control conditions, see Figure 5A, and for visualization of the global  
394 Higuchi fractal dimension for the psilocybin versus control conditions, see Figure 5B.



### Whole-brain Higuchi fractal dimension results.

Figure 5: The average Higuchi fractal dimension of BOLD time-series from every one of the 1,000 ROIs used in the Network Fractal Dimension section. Plot A corresponds to the LSD vs. LSD Control condition, Plot B corresponds to the Psilocybin vs. Psilocybin Control condition. For each time-series, the fractal dimension was calculated using a  $k_{max} = 64$ . While the effect size is small in absolute terms, given the small range that the fractal dimension of a time-series usually falls, it remains highly significant.

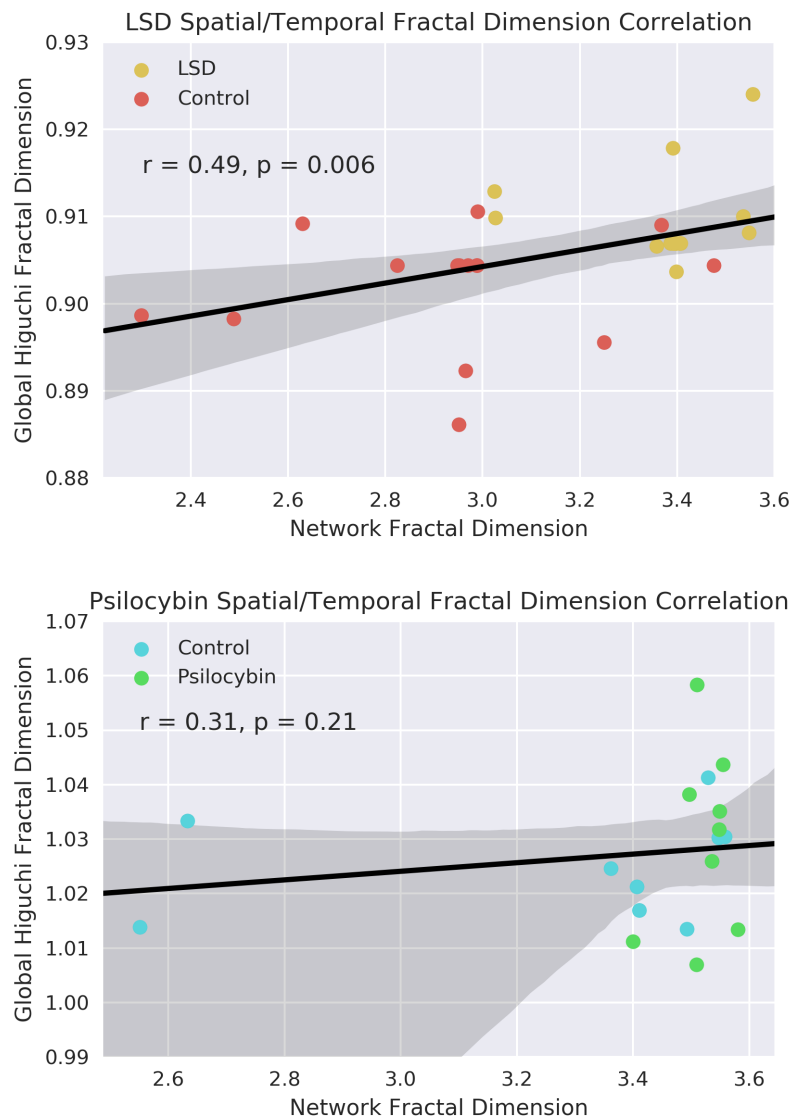
395

These results suggest that, at least for the LSD condition, the activity of the brain tends towards

396 increased fractal character in the temporal as well as spatial dimension. This is consistent with the  
397 EBH and serves as validation of the network fractal dimension results reported above. The difference  
398 between the averages between the two non-drug conditions (placebo condition of the LSD dataset,  
399 and the pre-infusion condition of the psilocybin dataset) are most likely explained by the significant  
400 difference in the lengths of scans and number of time-points the algorithm was fed. To test this,  
401 we re-ran the Higuchi fractal dimension analysis on LSD signals that had been truncated to be the  
402 same length as as the psilocybin time-series (100 samples), and found that there was no longer a  
403 significant difference between the drug and control conditions. We take this as evidence that the  
404 lack of significant difference between psilocybin and control conditions cannot be attributed to the  
405 drug directly but rather, may be reflective of a fundamental limitation in the utility of the Higuchi  
406 algorithm when working with sparse datasets.

407 We found a significant correlation between network fractal dimension and temporal fractal di-  
408 mension in the LSD condition ( $\rho = 0.49$ , p-value = 0.006), however, we did not find a significant  
409 correlation between the two metrics in the psilocybin conditions ( $\rho = 0.31$ , p-value = 0.21). For  
410 visualization, see Figure 6.





**Correlation between network fractal dimension and Higuchi fractal dimension.**

Figure 6: Correlation between network fractal dimension and global higuchi fractal dimension in the LSD and psilocybin conditions. In the LSD dataset, there was a significant, positive correlation between the two measures of fractal dimension ( $r=0.49$ ,  $p$ -value =  $0.006$ ) that was not apparent in the psilocybin dataset ( $r=0.23$ ,  $p$ -value = n.s.). As previously discussed, we believe this is reflective of the short length of the psilocybin time-series relative to the LSD scans.

### 411 **3.2.1 Localizing Time-Series Fractal Dimension to Sub-Networks**

412 To take advantage of the fact that the Higuchi method of calculating fractal dimension works on one  
413 time-series at a time, we were able to test whether any specific sub-networks of the brain displayed  
414 any changes in the fractal-dimension of the associated time-series. For the psilocybin condition,  
415 only one significant difference in the fractal dimension of BOLD time-series was found: the fractal  
416 dimension increased in the dorsal attentional network, at the edge of significance ( $H(6)$ ,  $p$ -value =  
417 0.05). In light of our suspicion that the psilocybin time-series are too short for meaningful Higuchi  
418 analysis, we strongly feel that these results should be replicated, using either longer fMRI scans, or,  
419 ideally, MEG or EEG data. For a table of the Higuchi fractal dimensions for each network tested in  
420 the psilocybin condition, see Table 1.

Sub-Network	Condition	BOLD Fractal Dimension	<i>p</i> -Value
Default-Mode Network	Control	1.023 ± 0.016	W(14)
	Psilocybin	1.032 ± 0.017	p = 0.31
Limbic Network	Control	1.034 ± 0.017	W(13)
	Psilocybin	1.044 ± 0.014	p = 0.26
Fronto-Parietal Network	Control	1.022 ± 0.021	W(17)
	Psilocybin	1.03 ± 0.018	p = 0.51
Somato-Motor Network	Control	1.031 ± 0.017	W(21)
	Psilocybin	1.028 ± 0.016	p = 0.86
Ventral-Attentional Network	Control	1.031 ± 0.018	W(21)
	Psilocybin	1.033 ± 0.02	p = 0.86
Dorsal-Attentional Network *	Control	1.013 ± 0.023	W(6)
	Psilocybin	1.027 ± 0.024	p = 0.05
Visual Network	Control	1.024 ± 0.025	W(17)
	Psilocybin	1.021 ± 0.027	p = 0.51

**Higuchi fractal dimension during psilocybin.**

Table 1: Higuchi fractal dimension of BOLD time-series from specific sub-networks in the Psilocybin vs. Control condition

\*  $p \leq 0.05$

\*\*  $p \leq 0.01$

\*\*\*  $p \leq 0.005$

421 For the LSD condition, compared to the placebo condition, we found significant increases in  
 422 fractal dimension under LSD in the fronto-parietal network (H(4), p-value = 0.001), in the dorsal-  
 423 attentional network (H(0), p-value=0.0005), and the visual network (H(4), p-value=0.001). For a  
 424 table of the Higuchi fractal dimensions for each network tested in the LSD condition, see Table 2.

Sub-Network	Condition	BOLD Fractal Dimension	<i>p</i> -Value
Default-Mode Network	LSD	0.906 ± 0.008	W(54)
	Control	0.905 ± 0.006	p = 0.73
Limbic Network	LSD	0.915 ± 0.006	W(57)
	Control	0.913 ± 0.009	p = 0.86
Fronto-Parietal Network ***	LSD	0.911 ± 0.009	W(4)
	Control	0.9 ± 0.001	p = 0.001
Somato-Motor Network	LSD	0.909 ± 0.006	W(45)
	Control	0.9 ± 0.012	p = 0.39
Ventral-Attentional Network	LSD	0.911 ± 0.007	W(58)
	Control	0.911 ± 0.007	p = 0.9
Dorsal Attentional Network ***	LSD	0.907 ± 0.009	W(0)
	Control	0.894 ± 0.007	0.0006
Visual Network ***	LSD	0.913 ± 0.003	W(4)
	Control	0.897 ± 0.013	p = 0.001

**Higuchi fractal dimension during LSD.**

Table 2: Higuchi fractal dimension of BOLD time-series from specific sub-networks in the LSD vs. Control condition

\*  $p \leq 0.05$

\*\*  $p \leq 0.01$

\*\*\*  $p \leq 0.005$

425 The significant increase in the dorsal-attentional network in both the LSD and psilocybin condi-  
426 tions suggests that this finding may be more robust than the increases in the fronto-parietal network  
427 or visual network that appear to be unique to LSD. An increase in the complexity of activity in the  
428 visual system under LSD is somewhat unsurprising, although why this did not appear in psilocybin  
429 is unclear (under the psilocybin condition the mean complexity in the visual system did increase  
430 relative to the pre-infusion condition, although this was not significant).

## 431 4 Discussion

432 Here, we report that, using a Compact-Box Burning algorithm [49], the fractal dimension of high-  
433 resolution cortical functional connectivity networks is increased under the influence of both psilocybin  
434 and LSD, both serotonergic psychedelic compounds, and that the fractal dimension of the BOLD  
435 time-series is increased by LSD, but not psilocybin. Furthermore, for both LSD and psilocybin, we  
436 were able to show a significant increase in the fractal dimension of the BOLD time-series in the  
437 brain regions generally thought to make up the dorsal-attentional network. These results suggest  
438 that psychedelic drugs increase the fractal character of brain activity in both temporal (as measured  
439 by Higuchi fractal dimension), and spatial domains (as measured by the Compact-Box burning  
440 algorithm). We interpret this result as an indicator that, under the influence of psychedelics, the  
441 brain moves towards a region of criticality [26, 27, 28], as fractal qualities emerge as the system  
442 nears a tipping point, or transition zone, from one phase into another [67]. This is in keeping with  
443 the predictions of the Entropic Brain Hypothesis (EBH), which hypothesizes that the level and  
444 quality of consciousness changes as the brain evolves towards the zone of criticality, between distinct  
445 phases [10, 4]. Our results also line up nicely with other attempts to quantify the complexity of  
446 brain activity under psychedelics, which have generally reported increases in entropy relative to an  
447 unaltered baseline [17, 16, 68, 20, 18].

448 One question that remains unanswered is what exactly the qualitative differences between those  
449 two phases might be: as was previously mentioned, the EBH intuitively lends itself to an Ising-like  
450 interpretation, where the critical moment partitions a low-entropy state and a more random, high-  
451 entropy phase, although this raises difficult questions about how that phase may present in a living,  
452 biological system. The critical Ising model has been used as a model for brain activity and may  
453 capture intrinsic properties of neural self-organization [29, 30, 31] An alternative model of criticality  
454 may be one of a branching process [69], where in the sub-critical regime the propagation of a branch  
455 is guaranteed to halt eventually, while in the super-critical regime, the branch flourishes, and at the  
456 point of criticality, the process branches into fractal patterns [70]. Simulations of neural networks  
457 suggest that super-critical behaviour should be epileptiform in nature [71], but psychedelics, on their  
458 own, do not typically induce seizures [72] (although collected anecdotal reports have suggested that

459 LSD, in combination with lithium can increase the risk of seizures [73], as can the the psilocybin  
460 analogue 5-methoxy-dimethyltryptamine [74]).

461 One interesting direction of research these results suggest is an analysis of whether the fractal  
462 dimension of a network, such as those explored here, encodes any information about the ability of  
463 that network to integrate information, a key issue of Integrated Information theory (IIT), [12, 13, 14].  
464 Simulations of small networks have found that the topology of a network can have implications for  
465 its capacity to act as an integrator of information [75]. In the cited simulation, network complexity  
466 was highest in a modular network based on the architecture of the visual system compared to  
467 a simpler, less integrated, network of the same type, or a network with a random distribution  
468 of connections. This idea of balancing integration and modularity recalls the findings by Gallos  
469 et al., that the fractal quality of functional connectivity networks plays a role in balancing these  
470 two competing topologies in a manner optimal for computation [44]. While it is computationally  
471 infeasible to do a crude calculation of integrated information for any non-trivial neural system due  
472 to the explosive growth in the number of computations involved, methods of estimating the value  
473 have been developed [76, 77], and so, using the fractal dimension analysis method described here, it  
474 should be possible to begin to explore whether there is a relationship between the fractal dimension  
475 of a system and it's ability to integrate information. Recently it has been shown that, in models  
476 of self-organizing, critical systems, such as Abelian sandpiles (which naturally tend towards critical  
477 states due to repeated build-up and relaxation of energy as the system evolves), critical behavior  
478 was surprisingly good at optimizing certain hard computational problems on graphs [78], suggesting  
479 that criticality may underlie some of the brain's own computational abilities.

480 While the theoretical implications for these results in the context of the EBH are interesting on  
481 their own, we also try to ground these results in the current literature concerning the neurobiology  
482 of psychedelic drugs. All serotonergic psychedelics (eg: LSD, mescaline, psilocybin) share agonist  
483 activity at the 5-HT<sub>2A</sub> receptor [79], a metabotropic serotonin receptor known to be involved in  
484 modulating a variety of behaviours. While the 5-HT<sub>2A</sub>r is widely expressed in the CNS, a specific  
485 population localized to Layer V pyramidal cells in the neocortex is both necessary and sufficient to  
486 induce psychedelic effects [80]. These Layer V pyramidal neurons serve as 'outputs' from one region  
487 of the cortex to another [81], and the 5-HT<sub>2A</sub>r acts as an excitatory receptor, decreasing polarization

488 and increasing the probability that a given neuron will fire [82, 83]. This suggests a primitive model  
489 of 5-HT<sub>2A</sub>r's role in neural information processing: on Layer V pyramidal neurons, the 5-HT<sub>2A</sub>r  
490 serves as a kind of 'information gate'. When a psychedelic is introduced to the brain, it binds to  
491 the 5-HT<sub>2A</sub>r, exciting the associated pyramidal neuron and decreasing the threshold required to  
492 successfully transmit information through the neuron. During normal waking consciousness, areas  
493 of the brain that are physically connected by Layer V pyramidal neurons may not be functionally  
494 connected because the signal threshold required to trigger an action potential is too high but when  
495 a psychedelic is introduced, that threshold goes down allowing novel patterns of information flow  
496 to occur. This perspective also recalls the branching process discussed above [69]. In this case,  
497 increasing the probability of a pyramidal neuron firing may be analogous to increasing the branching  
498 ratio  $\sigma$ , which, if  $\sigma$  is normally sub-critical, would bring the process closer to the critical value of  $\sigma_c$ .  
499 As networks with fractal topology are related to the trees generated by critical branching processes  
500 [70], this may be a fruitful area to explore further.

501 It is difficult to interpret the increase in the fractal dimension of the BOLD time-series in the  
502 dorsal-attentional network. This network is generally thought to be involved in a variety of processes  
503 related to visual processing of the environment, such as attending to the orientation of objects in  
504 space, visual feature-based attention, and biasing visual perception in response to cues [84]. It was  
505 originally proposed to be involved with top-down, conscious allocation of attention to environmental  
506 objects [85]. Human studies with psilocybin have found that exposure to the psychedelic reduces  
507 attentional tracking ability, and the proposed mechanism given was that psilocybin reduced the  
508 ability of the brain to filter out irrelevant or distracting stimuli [86]. This is consistent with find-  
509 ings that psychedelics attenuate sensory-gating functions in a manner reminiscent of patients with  
510 schizophrenia [87, 88].

511 The finding that LSD increased the fractal dimension of BOLD signals in the fronto-parietal  
512 network is consistent with previous findings that global increases in the functional connectivity  
513 density induced by LSD overlap with brain regions commonly assigned to the FP network [89].  
514 We did not, however find significant changes in the complexity of signals from nodes commonly  
515 assigned to the Default Mode Network (DMN), which ran counter to our initial hypothesis. Many  
516 neuroimaging studies of psilocybin and LSD have found associations between changes in DMN

517 activity and the phenomenology of the psychedelic experience [59, 58, 89, 90]. We hypothesize that  
518 this discrepancy might be explained by the sheer number of nodes assigned to the DMN (212 nodes  
519 in total): because the signal from every node was weighted equally, it is possible that peripheral  
520 nodes assigned to the DMN by our parcellation may not have been significantly effected, thus  
521 obscuring a real effect only present in a subset of DMN nodes. Validation with a smaller atlas or  
522 more conservative assignment of nodes may yet find an effect in the DMN (although a smaller atlas  
523 would preclude the NFD analysis).

524 Finally, the increased complexity of BOLD signals in the visual network under LSD is interesting,  
525 although perhaps unsurprising given the fantastically visual nature of the psychedelic experience.  
526 It has already been established that LSD alters functional connectivity of visual cortices in humans  
527 [91], and EEG analysis of LSD users post-experience has found alterations to the coherence of  
528 signals in visual areas thought to be associated with the experience of hallucinations [92]. It has  
529 been suggested that the qualitative nature of psychedelic imagery may be informative about the  
530 structure and layout of the visual system [93], and so we propose that this may be a particularly  
531 fruitful avenue of psychedelic research going forward.

532 This study has several limitations that are worth considering. The first is the comparatively  
533 small size of the psilocybin sample ( $n=9$ ), which means that it is harder to trust the replicability  
534 of the present findings than if the sample had been larger. Second, the Higuchi fractal dimension is  
535 not frequently used on BOLD signals, as the number of samples in each time-series is far lower than  
536 it is for EEG or MEG, resulting in a less robust analysis. In the case of psilocybin, the time-series  
537 may be so too short too produce Higuchi fractal dimension values of any reliability. In light of this,  
538 replication with EEG or MEG data should be a priority before these results are considered strong.  
539 Simultaneous EEG-fMRI recordings under a psychedelic would be particularly informative as it  
540 would enable us to test the relationship between fractal dimension recorded across modalities. Third,  
541 the parcellation resolution used here (1000 ROIs), which is considerably larger than many commonly-  
542 used parcellations is still smaller than would be desired for a truly comprehensive analysis of fractal  
543 dimension of functional connectivity networks, and so future analysis with a higher resolution cortical  
544 parcellation is needed. Future studies comparing different psychedelics, like LSD and psilocybin,  
545 should also strive to ensure some kind of dose-equivalence: given the nature of the datasets, it was



546 not possible to ensure that the subjective intensities of the LSD and psilocybin experiences volunteers  
547 underwent was equivalent, and this may be reflected in the differences in results. To control for this,  
548 it would be valuable to have a universal, standardized measure of subjective experience such as the  
549 ASC questionnaire [94], with graded doses for a variety of drugs, such as psilocybin, LSD, mescaline,  
550 etc. This would allow researchers the ability to more fully explore the commonalities, and differences  
551 between individual psychedelic compounds.

552 Finally, it is unclear what the functional, psychological implications of increased fractal prop-  
553 erties of brain activity and network organization are. Particularly profound subjective experiences  
554 under moderate-high doses of psychedelics are a highly reliable observation. Although there are  
555 clear differences in the specific vocabulary and intellectual framing used to describe and depict these  
556 experiences, variously referred to as peak experiences by some [95] and mystical-type experiences by  
557 others [96], there is clear consensus that the phenomenology of the experience itself is fundamental,  
558 and that its nature is often felt as exceptional in terms of both novelty and perceived meaning [7].  
559 Based on the present study's findings it is reasonable to speculate that the changes observed here,  
560 which are consistent with a system nearing criticality, may relate in some way to these profound  
561 subjective effects of psychedelics which include: exceptional sensitivity to environmental pertur-  
562 bation [97] and a sense of oneness or connectedness [98] including a sense of attunement to or  
563 aligned with nature [99, 97], referred to as the unitive experience [100] and thought to be a principal  
564 component of the peak/mystical-type experience [101]. The original EBH speculated that a closer  
565 tuning of brain activity to criticality may better reflect the ubiquitous criticality evident throughout  
566 the natural world and thus account for the subjective feeling of being better attuned to nature [10].  
567 Future work is now required to assess these speculative ideas and test the nature of the associations  
568 with greater specificity. This will demand improvements in sampling of the subjective experience  
569 [102] as much, if not more so, than improvements in the sampling of brain activity. Improving our  
570 understanding of the brain basis of the psychedelic experience may have implications for our under-  
571 standing of how these compounds might be best utilized, e.g. as aides to psychological development  
572 and therapy [10] as well as how they may model specific aspects of psychosis [103, 104].

## 573 **5 Conclusions**

574 In this study we report that, under the influence of two serotonergic psychedelics: LSD and psilo-  
575 cybin, the fractal dimension of cortical functional connectivity networks is significantly increased.  
576 Under LSD, the fractal dimension of BOLD time-series is also significantly increased, while psilo-  
577 cybin shows a non-significant increase as well. These results are in line with previously published  
578 research suggesting that psychedelics increase the complexity of brain activity, and the specific mea-  
579 sures used here may be a particularly useful tool for understanding how consciousness changes as  
580 the brain approaches criticality. We were able to show that, under both LSD and psilocybin, the  
581 fractal dimension of BOLD time-series from regions assigned to the dorsal-attentional network was  
582 increased. These findings show that psychedelics increase the fractal dimension of brain activity in  
583 both spatial and temporal domains and have implications for the study of consciousness and the  
584 neurobiology the psychedelic experience.

## 585 **Conflict of Interest Statement**

586 The authors report no personal or financial conflicts of interest related to the research reported  
587 herein.

## 588 **Acknowledgements**

589 The authors would like to thank the Cambridge University Department of Anaesthetics. We would  
590 like to specifically thank: Ioannis Pappas, Michael Craig, Dian Lu, and Andrea Luppi for their  
591 support. We would also like to thank Dr. Fernando Rosas for detailed feedback and insights.  
592 DK Menon is funded by the MRC, the NIHR Cambridge Biomedical Centre, and an NIHR Senior  
593 Investigator Award, and EA Stamatakis is funded by the Stephen Erskine Fellowship Queens College  
594 Cambridge. L Roseman has been supported by an Imperial President's Scholarship. Robin Carhart-  
595 Harris has been supported by the Beckley Foundation and is now supported by the Alex Mosley  
596 Charitable Trust and Ad Astria Chandaria Foundation. The original LSD research was completed  
597 with the support of a Wallacea.com crowd-funding campaign and the Beckley Foundation. The

598 psilocybin research was completed with the support of the Beckley Foundation and with additional  
599 support from the Neuro-psychoanalysis Foundation, Multidisciplinary Association for Psychedelic  
600 Studies, and the Heffter Research Institute.

## 601 **Author Contributions**

602 TFV, DKM and EAS carried out the research reported here. RC-H and LR designed the initial  
603 experiments, collected and preprocessed the data. TFV designed and performed the fractal analyses  
604 with feedback from EAS. TFV wrote the paper with feedback from all co-authors.

## 605 **References**

- 606 [1] Franz X. Vollenweider and Michael Kometer. The neurobiology of psychedelic drugs: impli-  
607 cations for the treatment of mood disorders. *Nature Reviews Neuroscience*, 11(9):642–651,  
608 September 2010.
- 609 [2] Kenneth W. Tupper, Evan Wood, Richard Yensen, and Matthew W. Johnson. Psychedelic  
610 medicine: a re-emerging therapeutic paradigm. *CMAJ: Canadian Medical Association journal*  
611 *= journal de l'Association medicale canadienne*, 187(14):1054–1059, October 2015.
- 612 [3] Andrew R. Gallimore. Restructuring consciousness the psychedelic state in light of integrated  
613 information theory. *Frontiers in Human Neuroscience*, 9, 2015.
- 614 [4] Robin L. Carhart-Harris. The entropic brain - revisited. *Neuropharmacology*, March 2018.
- 615 [5] Michael T. Alkire and Jason Miller. General anesthesia and the neural correlates of conscious-  
616 ness. *Progress in Brain Research*, 150:229–244, 2005.
- 617 [6] Erich Studerus, Michael Kometer, Felix Hasler, and Franz X. Vollenweider. Acute, suba-  
618 cute and long-term subjective effects of psilocybin in healthy humans: a pooled analysis of  
619 experimental studies. *Journal of Psychopharmacology*, 25(11):1434–1452, November 2011.

- 620 [7] R. R. Griffiths, W. A. Richards, U. McCann, and R. Jesse. Psilocybin can occasion mystical-  
621 type experiences having substantial and sustained personal meaning and spiritual significance.  
622 *Psychopharmacology*, 187(3):268–283, July 2006.
- 623 [8] Frederick S. Barrett and Roland R. Griffiths. Classic Hallucinogens and Mystical Experi-  
624 ences: Phenomenology and Neural Correlates. In *SpringerLink*, Current Topics in Behavioral  
625 Neurosciences, pages 1–38. Springer, Berlin, Heidelberg, 2017.
- 626 [9] Richard Evans Schultes, Albert Hofmann, and Christian Rtsch. *Plants of the Gods: Their*  
627 *Sacred, Healing, and Hallucinogenic Powers*. Inner Traditions/Bear, November 2001.
- 628 [10] Robin L. Carhart-Harris, Robert Leech, Peter J. Hellyer, Murray Shanahan, Amanda Feilding,  
629 Enzo Tagliazucchi, Dante R. Chialvo, and David Nutt. The entropic brain: a theory of con-  
630 scious states informed by neuroimaging research with psychedelic drugs. *Frontiers in Human*  
631 *Neuroscience*, 8, February 2014.
- 632 [11] Harry Eugene Stanley. *Introduction to Phase Transitions and Critical Phenomena*. Oxford  
633 University Press, 1987. Google-Books-ID: C3BzcUxoaNkC.
- 634 [12] Giulio Tononi. Consciousness as Integrated Information: a Provisional Manifesto. *The Bio-*  
635 *logical Bulletin*, 215(3):216–242, December 2008.
- 636 [13] G. Tononi. Integrated information theory of consciousness: An updated account. *Archives*  
637 *Italiennes de Biologie*, 150(2-3):56–90, 2012.
- 638 [14] Christof Koch, Marcello Massimini, Melanie Boly, and Giulio Tononi. Neural correlates of  
639 consciousness: progress and problems. *Nature Reviews Neuroscience*, 17(5):307–321, April  
640 2016.
- 641 [15] Naotsugu Tsuchiya, Shigeru Taguchi, and Hayato Saigo. Using category theory to assess the  
642 relationship between consciousness and integrated information theory. *Neuroscience Research*,  
643 107:1–7, June 2016.
- 644 [16] G. Petri, P. Expert, F. Turkheimer, R. Carhart-Harris, D. Nutt, P. J. Hellyer, and F. Vaccarino.

- 645 Homological scaffolds of brain functional networks. *Journal of the Royal Society, Interface /*  
646 *the Royal Society*, 11(101):20140873, December 2014.
- 647 [17] Enzo Tagliazucchi, Robin Carhart-Harris, Robert Leech, David Nutt, and Dante R. Chialvo.  
648 Enhanced repertoire of brain dynamical states during the psychedelic experience. *Human*  
649 *Brain Mapping*, 35(11):5442–5456, November 2014.
- 650 [18] A. Viol, Fernanda Palhano-Fontes, Heloisa Onias, Draulio B. Araujo, and G. M. Viswanathan.  
651 Shannon entropy of brain functional complex networks under the influence of the psychedelic  
652 Ayahuasca. *Scientific Reports*, 7(1):7388, August 2017.
- 653 [19] I. Pappas, R. M. Adapa, D. K. Menon, and E. A. Stamatakis. Brain network disintegration  
654 during sedation is mediated by the complexity of sparsely connected regions. *NeuroImage*,  
655 November 2018.
- 656 [20] Michael M. Schartner, Robin L. Carhart-Harris, Adam B. Barrett, Anil K. Seth, and Suresh D.  
657 Muthukumaraswamy. Increased spontaneous MEG signal diversity for psychoactive doses of  
658 ketamine, LSD and psilocybin. *Scientific Reports*, 7:46421, April 2017.
- 659 [21] Selen Atasoy, Leor Roseman, Mendel Kaelen, Morten L. Kringelbach, Gustavo Deco, and  
660 Robin L. Carhart-Harris. Connectome-harmonic decomposition of human brain activity reveals  
661 dynamical repertoire re-organization under LSD. *Scientific Reports*, 7(1):17661, December  
662 2017.
- 663 [22] Suresh D. Muthukumaraswamy and David T.J. Liley. 1/f electrophysiological spectra in resting  
664 and drug-induced states can be explained by the dynamics of multiple oscillatory relaxation  
665 processes. *NeuroImage*, 179:582–595, October 2018.
- 666 [23] Benoit Mandelbrot. The Fractal Geometry of Nature. In *American Journal of Physics*, vol-  
667 ume 51, page 468 p. March 1983.
- 668 [24] Falconer Kenneth. Fractal geometry. UK: WILEY, 337, 2003.
- 669 [25] David G. Tarboton, Rafael L. Bras, and Ignacio RodriguezIturbe. The fractal nature of river  
670 networks. *Water Resources Research*, 24(8):1317–1322, August 1988.

- 671 [26] Per Bak, Chao Tang, and Kurt Wiesenfeld. Self-organized criticality: An explanation of the  
672  $1/f$  noise. *Physical Review Letters*, 59(4):381–384, July 1987.
- 673 [27] Akitomo Watanabe, Shogo Mizutaka, and Kousuke Yakubo. Fractal and Small-World Net-  
674 works Formed by Self-Organized Critical Dynamics. *Journal of the Physical Society of Japan*,  
675 84(11):114003, October 2015.
- 676 [28] Shogo Mizutaka. Simple model of fractal networks formed by self-organized critical dynamics.  
677 *arXiv:1806.05397 [nlin, physics:physics, q-bio]*, June 2018. arXiv: 1806.05397.
- 678 [29] Ariel Haimovici, Enzo Tagliazucchi, Pablo Balenzuela, and Dante R. Chialvo. Brain Organiza-  
679 tion into Resting State Networks Emerges at Criticality on a Model of the Human Connectome.  
680 *Physical Review Letters*, 110(17):178101, April 2013.
- 681 [30] T. K. Das, P. M. Abeyasinghe, J. S. Crone, A. Sosnowski, S. Laureys, A. M. Owen, and  
682 A. Soddu. Highlighting the Structure-Function Relationship of the Brain with the Ising Model  
683 and Graph Theory. *BioMed Research International*, 2014, 2014.
- 684 [31] Pubuditha M. Abeyasinghe, Demetrius Ribeiro de Paula, Sina Khajehabdollahi, Sree Ram  
685 Valluri, Adrian M. Owen, and Andrea Soddu. Role of Dimensionality in Predicting the Sponta-  
686 neous Behavior of the Brain Using the Classical Ising Model and the Ising Model Implemented  
687 on a Structural Connectome. *Brain Connectivity*, 8(7):444–455, June 2018.
- 688 [32] R. B. Stinchcombe. Fractals, phase transitions and criticality. *Proc. R. Soc. Lond. A*,  
689 423(1864):17–33, May 1989.
- 690 [33] W Klonowski, E Olejarczyk, and R Stepień. Sleep-EEG Analysis Using Higuchi's Fractal  
691 Dimension. page 4, Bruges, Belgium, October 2005. NOLTA2005.
- 692 [34] Włodzisław Klonowski, Paweł Stepień, and Robert Stepień. Complexity Measures of Brain  
693 Electrophysiological Activity. *Journal of Psychophysiology*, 24(2):131–135, January 2010.
- 694 [35] Sladjana Spasic, Srdjan Kesic, Aleksandar Kalauzi, and Jasna Saponjic. Different anesthesia  
695 in rat induces distinct inter-structure brain dynamic detected by higuchi fractal dimension.  
696 *Fractals*, 19(01):113–123, March 2011.

- 697 [36] Paul Hejja and Samuel Galloon. A consideration of ketamine dreams. *Canadian Anaesthetists*  
698 *Society Journal*, 22(1):100, January 1975.
- 699 [37] Antonio Ieva, Fabio Grizzi, Herbert Jelinek, Andras J. Pellionisz, and Gabriele Angelo Losa.  
700 Fractals in the Neurosciences, Part I: General Principles and Basic Neurosciences. *The Neuro-*  
701 *scientist: A Review Journal Bringing Neurobiology, Neurology and Psychiatry*, 20(4):403–417,  
702 August 2014.
- 703 [38] Antonio Di Ieva, Francisco J. Esteban, Fabio Grizzi, Wlodzimierz Klonowski, and Miguel  
704 Martn-Landrove. Fractals in the Neurosciences, Part II: Clinical Applications and Future  
705 Perspectives. *The Neuroscientist*, 21(1):30–43, February 2015.
- 706 [39] Tae Hyon Ha, Uicheul Yoon, Kyung Jin Lee, Yong Wook Shin, Jong-Min Lee, In Young Kim,  
707 Kyoo Seob Ha, Sun I. Kim, and Jun Soo Kwon. Fractal dimension of cerebral cortical surface in  
708 schizophrenia and obsessivecompulsive disorder. *Neuroscience Letters*, 384(1):172–176, August  
709 2005.
- 710 [40] Kiho Im, Jong-Min Lee, Uicheul Yoon, Yong-Wook Shin, Soon Beom Hong, In Young Kim,  
711 Jun Soo Kwon, and Sun I. Kim. Fractal dimension in human cortical surface: multiple regres-  
712 sion analysis with cortical thickness, sulcal depth, and folding area. *Human Brain Mapping*,  
713 27(12):994–1003, December 2006.
- 714 [41] Richard D. King, Anuh T. George, Tina Jeon, Linda S. Hynan, Teddy S. Youn, David N.  
715 Kennedy, and Bradford Dickerson. Characterization of Atrophic Changes in the Cerebral  
716 Cortex Using Fractal Dimensional Analysis. *Brain imaging and behavior*, 3(2):154–166, June  
717 2009.
- 718 [42] Nazahah Mustafa, Trevor S. Ahearn, Gordon D. Waiter, Alison D. Murray, Lawrence J. Whal-  
719 ley, and Roger T. Staff. Brain structural complexity and life course cognitive change. *Neu-*  
720 *roImage*, 61(3):694–701, July 2012.
- 721 [43] Lazaros Gallos, Mariano Sigman, and Hernan Makse. The Conundrum of Functional Brain  
722 Networks: Small-World Efficiency or Fractal Modularity. *Frontiers in Physiology*, 3, 2012.

- 723 [44] Lazaros K. Gallos, Hernn A. Makse, and Mariano Sigman. A small world of weak ties provides  
724 optimal global integration of self-similar modules in functional brain networks. *Proceedings of*  
725 *the National Academy of Sciences*, 109(8):2825–2830, February 2012.
- 726 [45] Alfrd Renyi. On Measures of Entropy and Information. Berkeley, CA, 1961. The Regents of  
727 the University of California.
- 728 [46] Oldrich Zmeskal, Petr Dzik, and Michal Vesely. Entropy of fractal systems. *Computers &*  
729 *Mathematics with Applications*, 66(2):135–146, August 2013.
- 730 [47] A. Renyi. On the dimension and entropy of probability distributions. *Acta Mathematica*  
731 *Academiae Scientiarum Hungarica*, 10(1-2):193–215, March 1959.
- 732 [48] Daijun Wei, Bo Wei, Yong Hu, Haixin Zhang, and Yong Deng. A new information dimension  
733 of complex networks. *Physics Letters A*, 378(16):1091–1094, March 2014.
- 734 [49] Chaoming Song, Lazaros K. Gallos, Shlomo Havlin, and Hernan A. Makse. How to calculate  
735 the fractal dimension of a complex network: the box covering algorithm. *Journal of Statistical*  
736 *Mechanics: Theory and Experiment*, 2007(03):P03006–P03006, March 2007. arXiv: cond-  
737 mat/0701216.
- 738 [50] T. Higuchi. Approach to an irregular time series on the basis of the fractal theory. *Physica D:*  
739 *Nonlinear Phenomena*, 31(2):277–283, June 1988.
- 740 [51] B. Mandelbrot. How long is the coast of britain? Statistical self-similarity and fractional  
741 dimension. *Science (New York, N.Y.)*, 156(3775):636–638, May 1967.
- 742 [52] Joost J. Joosten, Fernando Soler-Toscano, and Hector Zenil. Fractal Dimension versus Process  
743 Complexity. *Advances in Mathematical Physics*, 2016.
- 744 [53] A. Clauset, C. Shalizi, and M. Newman. Power-Law Distributions in Empirical Data. *SIAM*  
745 *Review*, 51(4):661–703, November 2009.
- 746 [54] Srdjan Kesi and Sladjana Z. Spasi. Application of Higuchi’s fractal dimension from basic to  
747 clinical neurophysiology: A review. *Computer Methods and Programs in Biomedicine*, 133:55–  
748 70, September 2016.



- 749 [55] Michael Schartner, Anil Seth, Quentin Noirhomme, Melanie Boly, Marie-Aurelie Bruno, Steven  
750 Laureys, and Adam Barrett. Complexity of Multi-Dimensional Spontaneous EEG Decreases  
751 during Propofol Induced General Anaesthesia. *PLOS ONE*, 10(8):e0133532, August 2015.
- 752 [56] Michael M. Schartner, Andrea Pigorini, Steve A. Gibbs, Gabriele Arnulfo, Simone Sarasso,  
753 Lionel Barnett, Lino Nobili, Marcello Massimini, Anil K. Seth, and Adam B. Barrett. Global  
754 and local complexity of intracranial EEG decreases during NREM sleep. *Neuroscience of*  
755 *Consciousness*, 2017(1), January 2017.
- 756 [57] Forrest Sheng Bao, Xin Liu, and Christina Zhang. PyEEG: An Open Source Python Module  
757 for EEG/MEG Feature Extraction. *Computational Intelligence and Neuroscience*, 2011, 2011.
- 758 [58] Robin L. Carhart-Harris, Suresh Muthukumaraswamy, Leor Roseman, Mendel Kaelen, Wouter  
759 Droog, Kevin Murphy, Enzo Tagliazucchi, Eduardo E. Schenberg, Timothy Nest, Csaba Or-  
760 ban, Robert Leech, Luke T. Williams, Tim M. Williams, Mark Bolstridge, Ben Sessa, John  
761 McGonigle, Martin I. Sereno, David Nichols, Peter J. Hellyer, Peter Hobden, John Evans,  
762 Krish D. Singh, Richard G. Wise, H. Valerie Curran, Amanda Feilding, and David J. Nutt.  
763 Neural correlates of the LSD experience revealed by multimodal neuroimaging. *Proceedings of*  
764 *the National Academy of Sciences*, page 201518377, April 2016.
- 765 [59] Robin L. Carhart-Harris, David Erritzoe, Tim Williams, James M. Stone, Laurence J. Reed,  
766 Alessandro Colasanti, Robin J. Tyacke, Robert Leech, Andrea L. Malizia, Kevin Murphy,  
767 Peter Hobden, John Evans, Amanda Feilding, Richard G. Wise, and David J. Nutt. Neural  
768 correlates of the psychedelic state as determined by fMRI studies with psilocybin. *Proceedings*  
769 *of the National Academy of Sciences*, 109(6):2138–2143, February 2012.
- 770 [60] Susan Whitfield-Gabrieli and Alfonso Nieto-Castanon. Conn: a functional connectivity toolbox  
771 for correlated and anticorrelated brain networks. *Brain Connectivity*, 2(3):125–141, 2012.
- 772 [61] Alexander Schaefer, Ru Kong, Evan M. Gordon, Timothy O. Laumann, Xi-Nian Zuo, Avram J.  
773 Holmes, Simon B. Eickhoff, and B. T. Thomas Yeo. Local-Global Parcellation of the Human  
774 Cerebral Cortex from Intrinsic Functional Connectivity MRI. *Cerebral Cortex (New York,*  
775 *N.Y.: 1991)*, pages 1–20, July 2017.

- 776 [62] B. T. Yeo, Fenna M. Krienen, Jorge Sepulcre, Mert R. Sabuncu, Danial Lashkari, Marisa  
777 Hollinshead, Joshua L. Roffman, Jordan W. Smoller, Lilla Zllel, Jonathan R. Polimeni, Bruce  
778 Fischl, Hesheng Liu, and Randy L. Buckner. The organization of the human cerebral cortex  
779 estimated by intrinsic functional connectivity. *Journal of Neurophysiology*, 106(3):1125–1165,  
780 September 2011.
- 781 [63] Stfan van der Walt, S. Chris Colbert, and Gal Varoquaux. The NumPy Array: A Structure for  
782 Efficient Numerical Computation. *Computing in Science & Engineering*, 13(2):22–30, March  
783 2011.
- 784 [64] Eric Jones, Travis Oliphant, and Pearu Peterson. SciPy: Open Source Scientific Tools for  
785 Python. January 2001.
- 786 [65] Aric Hagberg, Daniel Schult, and Pieter Swart. Exploring Network Structure, Dynamics, and  
787 Function using NetworkX. 2008.
- 788 [66] Yoav Benjamini and Yosef Hochberg. Controlling the False Discovery Rate: A Practical and  
789 Powerful Approach to Multiple Testing. *Journal of the Royal Statistical Society. Series B*  
790 *(Methodological)*, 57(1):289–300, 1995.
- 791 [67] John M. Beggs and Nicholas Timme. Being Critical of Criticality in the Brain. *Frontiers in*  
792 *Physiology*, 3, 2012.
- 793 [68] A.v. Lebedev, M. Kaelin, M. Lvdn, J. Nilsson, A. Feilding, D.j. Nutt, and R.l. Carhart-  
794 Harris. LSD-induced entropic brain activity predicts subsequent personality change. *Human*  
795 *Brain Mapping*, 37(9):3203–3213, September 2016.
- 796 [69] Mikko Alava and Kent Lauritsen. Branching Processes. In *Encyclopedia of Complexity and*  
797 *Systems Science*. 2009.
- 798 [70] K-I Goh, G Salvi, B Kahng, and D Kim. Skeleton and Fractal Scaling in Complex Networks.  
799 *Physical Review Letters*, 96, 2006.
- 800 [71] David Hsu, Wei Chen, Murielle Hsu, and John M. Beggs. An open hypothesis: is epilepsy  
801 learned, and can it be unlearned? *Epilepsy & behavior : E&B*, 13(3):511–522, October 2008.

- 802 [72] P. G. Zagnoni and C. Albano. Psychostimulants and epilepsy. *Epilepsia*, 43 Suppl 2:28–31,  
803 2002.
- 804 [73] Mike Brown. Interactions Between LSD and Antidepressants, October 2003.
- 805 [74] Shaun L. Greene. Chapter 15 - Tryptamines. In Paul I. Dargan and David M. Wood, editors,  
806 *Novel Psychoactive Substances*, pages 363–381. Academic Press, Boston, January 2013.
- 807 [75] G. Tononi, O. Sporns, and G. M. Edelman. A measure for brain complexity: relating functional  
808 segregation and integration in the nervous system. *Proceedings of the National Academy of  
809 Sciences*, 91(11):5033–5037, May 1994.
- 810 [76] Max Tegmark. Improved Measures of Integrated Information. *PLOS Computational Biology*,  
811 12(11):e1005123, November 2016.
- 812 [77] Hyoungkyu Kim, Anthony G. Hudetz, Joseph Lee, George A. Mashour, UnCheol Lee, the ReC-  
813 Cognition Study Group, Michael S. Avidan, Tarik Bel-Bahar, Stefanie Blain-Moraes, Goodarz  
814 Golmirzaie, Ellen Janke, Max B. Kelz, Paul Picton, Vijay Tarnal, Giancarlo Vanini, and  
815 Phillip E. Vlisides. Estimating the Integrated Information Measure Phi from High-Density  
816 Electroencephalography during States of Consciousness in Humans. *Frontiers in Human Neu-  
817 roscience*, 12, 2018.
- 818 [78] Heiko Hoffmann and David W. Payton. Optimization by Self-Organized Criticality. *Scientific  
819 Reports*, 8(1):2358, February 2018.
- 820 [79] David E. Nichols. Psychedelics. *Pharmacological Reviews*, 68(2):264–355, April 2016.
- 821 [80] Javier Gonzalez-Maeso, Noelia V. Weisstaub, Mingming Zhou, Pokman Chan, Lidija Ivic, Ros-  
822 alind Ang, Alena Lira, Maria Bradley-Moore, Yongchao Ge, Qiang Zhou, Stuart C. Sealton,  
823 and Jay A. Gingrich. Hallucinogens recruit specific cortical 5-HT(2a) receptor-mediated sig-  
824 naling pathways to affect behavior. *Neuron*, 53(3):439–452, February 2007.
- 825 [81] Nelson Spruston. Pyramidal neurons: dendritic structure and synaptic integration. *Nature  
826 Reviews. Neuroscience*, 9(3):206–221, March 2008.

- 827 [82] Rodrigo Andrade. Serotonergic regulation of neuronal excitability in the prefrontal cortex.  
828 *Neuropharmacology*, 61(3):382–386, September 2011.
- 829 [83] Daniel Avesar and Allan T. Gullledge. Selective serotonergic excitation of callosal projection  
830 neurons. *Frontiers in Neural Circuits*, 6:12, 2012.
- 831 [84] Simone Vossel, Joy J. Geng, and Gereon R. Fink. Dorsal and Ventral Attention Systems. *The  
832 Neuroscientist*, 20(2):150–159, April 2014.
- 833 [85] Maurizio Corbetta and Gordon L. Shulman. Control of goal-directed and stimulus-driven  
834 attention in the brain. *Nature Reviews. Neuroscience*, 3(3):201–215, March 2002.
- 835 [86] Olivia L. Carter, David C. Burr, John D. Pettigrew, Guy M. Wallis, Felix Hasler, and Franz X.  
836 Vollenweider. Using psilocybin to investigate the relationship between attention, working mem-  
837 ory, and the serotonin 1a and 2a receptors. *Journal of Cognitive Neuroscience*, 17(10):1497–  
838 1508, October 2005.
- 839 [87] Jordi Riba, Antoni Rodriguez-Fornells, and Manel J. Barbanoj. Effects of ayahuasca on sensory  
840 and sensorimotor gating in humans as measured by P50 suppression and prepulse inhibition  
841 of the startle reflex, respectively. *Psychopharmacology*, 165(1):18–28, December 2002.
- 842 [88] Franz X. Vollenweider, Philipp A. Csomor, Bernhard Knappe, Mark A. Geyer, and Boris B.  
843 Quednow. The effects of the preferential 5-HT<sub>2a</sub> agonist psilocybin on prepulse inhibition of  
844 startle in healthy human volunteers depend on interstimulus interval. *Neuropsychopharmacol-  
845 ogy: Official Publication of the American College of Neuropsychopharmacology*, 32(9):1876–  
846 1887, September 2007.
- 847 [89] Enzo Tagliazucchi, Leor Roseman, Mendel Kaelen, Csaba Orban, SureshD. Muthuku-  
848 maraswamy, Kevin Murphy, Helmut Laufs, Robert Leech, John McGonigle, Nicolas Crossley,  
849 Edward Bullmore, Tim Williams, Mark Bolstridge, Amanda Feilding, DavidJ. Nutt, and Robin  
850 Carhart-Harris. Increased Global Functional Connectivity Correlates with LSD-Induced Ego  
851 Dissolution. *Current Biology*, 26(8):1043–1050, April 2016.
- 852 [90] Matthew Wall. Psilocybin for treatment-resistant depression: fMRI-measured brain mecha-  
853 nisms. *Scientific Reports*, 7, October 2017.

- 854 [91] Leor Roseman, Martin I. Sereno, Robert Leech, Mendel Kaelen, Csaba Orban, John McGo-  
855 ngle, Amanda Feilding, David J. Nutt, and Robin L. CarhartHarris. LSD alters eyes-closed  
856 functional connectivity within the early visual cortex in a retinotopic fashion. *Human Brain*  
857 *Mapping*, 37(8):3031–3040, April 2016.
- 858 [92] H. D. Abraham and F. H. Duffy. EEG coherence in post-LSD visual hallucinations. *Psychiatry*  
859 *Research*, 107(3):151–163, October 2001.
- 860 [93] Paul C. Bressloff, Jack D. Cowan, Martin Golubitsky, Peter J. Thomas, and Matthew C.  
861 Wiener. What geometric visual hallucinations tell us about the visual cortex. *Neural Compu-*  
862 *tation*, 14(3):473–491, March 2002.
- 863 [94] Matthias E. Liechti. Modern Clinical Research on LSD. *Neuropsychopharmacology: Official*  
864 *Publication of the American College of Neuropsychopharmacology*, 42(11):2114–2127, October  
865 2017.
- 866 [95] Leor Roseman, David J. Nutt, and Robin L. Carhart-Harris. Quality of Acute Psychedelic  
867 Experience Predicts Therapeutic Efficacy of Psilocybin for Treatment-Resistant Depression.  
868 *Frontiers in Pharmacology*, 8, 2018.
- 869 [96] Katherine A. MacLean, Matthew W. Johnson, and Roland R. Griffiths. Mystical Experiences  
870 Occasioned by the Hallucinogen Psilocybin Lead to Increases in the Personality Domain of  
871 Openness. *Journal of psychopharmacology (Oxford, England)*, 25(11):1453–1461, November  
872 2011.
- 873 [97] Robin L. Carhart-Harris, Leor Roseman, Eline Haijen, David Erritzoe, Rosalind Watts, Igor  
874 Branchi, and Mendel Kaelen. Psychedelics and the essential importance of context. *Journal*  
875 *of Psychopharmacology (Oxford, England)*, 32(7):725–731, 2018.
- 876 [98] Rosalind Watts, Camilla Day, Jacob Krzanowski, David Nutt, and Robin Carhart-Harris.  
877 Patients Accounts of Increased Connectedness and Acceptance After Psilocybin for Treatment-  
878 Resistant Depression. *Journal of Humanistic Psychology*, 57(5):520–564, September 2017.

- 879 [99] Taylor Lyons and Robin L. Carhart-Harris. Increased nature relatedness and decreased au-  
880 thoritarian political views after psilocybin for treatment-resistant depression. *Journal of Psy-*  
881 *chopharmacology (Oxford, England)*, 32(7):811–819, July 2018.
- 882 [100] Walter Terence Stace and Walter T. Stace. *Mysticism and Philosophy*. J.P. Tarcher, 1987.  
883 Google-Books-ID: OM54AAAAMAAJ.
- 884 [101] Walter N. Pahnke and William A. Richards. Implications of LSD and experimental mysticism.  
885 *Journal of Religion and Health*, 5(3):175–208, July 1966.
- 886 [102] Jonathan Smallwood and Jonathan W. Schooler. The Science of Mind Wandering: Empirically  
887 Navigating the Stream of Consciousness. *Annual Review of Psychology*, 66(1):487–518, 2015.
- 888 [103] RL Carhart-Harris, S Brugger, DJ Nutt, and JM Stone. Psychiatry's next top model: cause  
889 for a re-think on drug models of psychosis and other psychiatric disorders. *Journal of Psy-*  
890 *chopharmacology*, 27(9):771–778, September 2013.
- 891 [104] Hannah Steeds, Robin L. Carhart-Harris, and James M. Stone. Drug models of schizophrenia.  
892 *Therapeutic Advances in Psychopharmacology*, 5(1):43–58, February 2015.